Vascular patterns in the heads of crocodilians: blood vessels and sites of thermal exchange

William Ruger Porter,[1] Jayc C. Sedlmayr[2] and Lawrence M. Witmer[1]

[1]*Department of Biomedical Sciences, Ohio University Heritage College of Osteopathic Medicine, Athens, OH, USA*
[2]*Department of Cell Biology and Anatomy, Louisiana State University Heath Sciences Center, New Orleans, LA, USA*

Abstract

Extant crocodilians are a highly apomorphic archosaur clade that is ectothermic, yet often achieve large body sizes that can be subject to higher heat loads. Therefore, the anatomical and physiological roles that blood vessels play in crocodilian thermoregulation need further investigation to better understand how crocodilians establish and maintain cephalic temperatures and regulate neurosensory tissue temperatures during basking and normal activities. The cephalic vascular anatomy of extant crocodilians, particularly American alligator (*Alligator mississippiensis*) was investigated using a differential-contrast, dual-vascular injection technique and high resolution X-ray micro-computed tomography (μCT). Blood vessels were digitally isolated to create representations of vascular pathways. The specimens were then dissected to confirm CT results. Sites of thermal exchange, consisting of the oral, nasal, and orbital regions, were given special attention due to their role in evaporative cooling and cephalic thermoregulation in other diapsids. Blood vessels to and from sites of thermal exchange were studied to detect conserved vascular patterns and to assess their ability to deliver cooled blood to neurosensory tissues. Within the orbital region, both the arteries and veins demonstrated consistent branching patterns, with the supraorbital, infraorbital, and ophthalmotemporal vessels supplying and draining the orbit. The venous drainage of the orbital region showed connections to the dural sinuses via the orbital veins and cavernous sinus. The palatal region demonstrated a vast plexus that comprised both arteries and veins. The most direct route of venous drainage of the palatal plexus was through the palatomaxillary veins, essentially bypassing neurosensory tissues. Anastomotic connections with the nasal region, however, may provide an alternative route for palatal venous blood to reach neurosensory tissues. The nasal region in crocodilians is probably the most prominent site of thermal exchange, as it offers a substantial surface area and is completely surrounded by blood vessels. The venous drainage routes from the nasal region offer routes directly to the dural venous sinuses and the orbit, offering evidence of the potential to directly affect neurosensory tissue temperatures. The evolutionary history of crocodilians is complex, with large-bodied, terrestrial, and possibly endothermic taxa that may have had to deal with thermal loads that likely provided the anatomical building-blocks for such an extensive vascularization of sites of thermal exchange. A clear understanding of the physiological abilities and the role of blood vessels in the thermoregulation of crocodilians neurosensory tissues is not available but vascular anatomical patterns of crocodilian sites of thermal exchange indicate possible physiological abilities that may be more sophisticated than in other extant diapsids.

Key words: blood vessels; cephalic; crocodilian; thermoregulation; vasculature.

Introduction

Research into the cephalic vasculature of crocodilians has, unfortunately, not received the same level of scrutiny as

have that of birds, squamates, or mammals. The available published research is over 100 years old (Rathke, 1866; Hochstetter, 1906; Reese, 1914, 1915), with the exception of Sedlmayr's (2002) extensive investigation into the vascular anatomy of extant crocodilians and Almeida & Campos's (2011) work on encephalic arteries. Determining the role of blood vessels in cephalic physiological thermoregulation is crucial for understanding how crocodilians regulate brain temperature. Selective brain temperature regulation has been demonstrated in squamates (Heath, 1964, 1966;

Correspondence
William Ruger Porter, Department of Biomedical Sciences, Ohio University, 228 Irvine Hall, Athens, OH 45701, USA.
T: + 1 740 3312694; E: porterw1@ohio.edu

Crawford, 1972; Crawford et al. 1977), birds (Kilgore et al. 1976; Bernstein et al. 1979), and mammals (Mitchell et al. 1997, 2002), and thus is expected on phylogenetic grounds in crocodilians. Indeed, physiological thermoregulation in the head has been investigated to some degree in crocodilians. For example, Johnson (1974) reported that a temperature differential between the head and body occurs in crocodilians such that, similar to other reptiles (Crawford, 1972), the head warms slower than the body under certain conditions, especially during gaping. The number of publications focusing on behavioral thermoregulation in crocodilians is high (Smith, 1976, 1979; Drane et al. 1977; Smith et al. 1978, 1984; Fraser & Grigg, 1984; Franklin & Seebacher, 2003; Seebacher & Franklin, 2004, 2007) and it is well understood how crocodilians control body temperature during warming and cooling. Yet, similar to squamates, crocodilians have distinct vascular abilities that are directly related to adjusting body temperatures and, like other reptiles, may have evolved a circulatory system that elevates a function in thermoregulation over oxygen delivery (Pough, 1980; Seebacher & Franklin, 2004, 2007). Crocodilians have also been shown to vasodilate peripheral blood vessels and increase heart rate to increase temperature quickly and to vasoconstrict peripheral blood vessels and reduce heart rate to slow the shedding of heat and maintain body temperature (Smith, 1976, 1979; Drane et al. 1977; Smith et al. 1978; Franklin & Seebacher, 2003; Seebacher & Franklin, 2004, 2007). The number of publications investigating physiological sites of heat exchange is small. Spotila et al. (1977) and Smith (1979) indicated that gaping during basking influences head temperature by exposing the oral region and implies that evaporative cooling occurs within the oral cavity. It is unknown whether this behavior is an active attempt to control head temperature during basking or to assert more control over behavioral thermoregulation. Extending basking times would allow larger individuals to warm to a preferred body temperature without increasing head or neurosensory tissue temperatures (Smith, 1979).

To our knowledge, no study has directly investigated the influence of the highly vascularized crocodilian nasal and orbital regions on head or brain temperatures. Much of the research has focused on the thermoregulatory abilities of endotherms, like birds (Kilgore et al. 1976; Bernstein et al. 1979) and mammals (Mitchell et al. 1997), which are thought to require close regulation of brain temperature due to their constant and elevated body temperatures being close to lethal temperatures (Colbert et al. 1946). Ectotherms, in contrast, may have evolved a circulatory system that is, in some ways, much more sophisticated than that of endotherms, with roles in physiological processes that actively increase and sustain body temperatures (Pough, 1980; Franklin & Seebacher, 2003; Seebacher & Franklin, 2004, 2007). Given the number of publications focusing on body temperature, thermoregulation, and

vascular physiological abilities in other diapsids, it is likely that crocodilians also use blood vessels to regulate the temperature of the head, specifically the temperature of neurosensory tissues (brain, eye, etc.). This study seeks to understand the vascular anatomy of key areas of the head (e.g. the oral, nasal, and orbital regions) that are known to have a role in heat exchange in birds (Midtgård, 1983) and squamates (Templeton, 1960).

Knowledge of crocodilian cephalic vasculature also serves a critical role in inferring the vascular anatomy and physiology of dinosaurs as crocodilians are only one of two extant archosaur clades. Conversely, crocodilians and birds are divergently apomorphic clades that offer some challenges to the study of dinosaur vascular anatomy. For example, crocodilians display a dramatic facial rotation that flattens the skull (Witmer, 1995b, 1997), a reduction of the antorbital sinus (Witmer, 1995b), a secondary bony palate that extends from the nasal cavity into the pterygoid bone (Ferguson, 1981), and suturing of the quadrate and pterygoid to the braincase (Witmer, 1995b; Sedlmayr, 2002). Moreover, there are documented differences among crocodilians in thermoregulatory abilities that relate to body size (Smith, 1979; Fraser & Grigg, 1984; Smith et al. 1984). Thus, crocodilians may have a bearing for inferring some of the effects of size on dinosaur thermoregulatory strategies, in that these studies may provide insight into both the problems and solutions of how large and small nonavian dinosaurs thermoregulated (Seebacher et al. 1999). Birds, in contrast to crocodilians, are endothermic, have enlarged eyeballs and brains, expanded nasal vestibules, reduced maxillae, and show fusion of several skull bones. Despite these divergent morphological conditions, extant archosaurs have shown similar vascular patterns (Sedlmayr, 2002; Porter, 2015).

This study seeks: (i) to investigate the vascular anatomy of crocodilians to understand blood vessels that could play a role in influencing head temperature; (ii) to document anatomical patterns, routes of blood flow, pathways to and from sites of thermal exchange; and (iii) to detect and describe vascular osteological correlates (e.g. foramina, grooves, canals; Witmer, 1995a). The amount of vascular variation was observed with special attention to osteological correlates to ensure that these bony signatures are consistently produced by homologous blood vessels. The nomenclature in this study largely follows that of Sedlmayr (2002).

Materials and methods

Eight cadaveric specimens of *Alligator mississippiensis* were obtained from the Rockefeller Wildlife Refuge (Fig. 1). These alligator specimens supplement the sample used by Sedlmayr (2002), and many of the specimens in that sample remained available for this study. One specimen of subadult *Crocodylus johnsoni* [Ohio University Vertebrate Collection (OUVC) 10426] was obtained from the St.

Augustine Zoological Gardens. Specimens were studied using vascular injection, CT scanning (Fig. 2), and gross dissection. All specimens were frozen for variable periods of time prior to analysis and subsequently thawed prior to injection. None were embalmed or otherwise fixed prior to injection. Each specimen was scanned prior to vascular injection at the Ohio University MicroCT Scanning Facility (OUμCT) on a GE eXplore Locus *in vivo* Small Animal MicroCT scanner at 45 and 90 μm slice thicknesses, 80 kV, 450 μA. The carotid arteries and internal jugular veins were cannulated with a 20-gauge cannula (Becton Dickinson and Co., Franklin Lakes, NJ, USA) and injected with a solution of colored latex (Ward's, Rochester, NY, USA) and barium (E-Z-EM, Westbury, NY, USA) using the
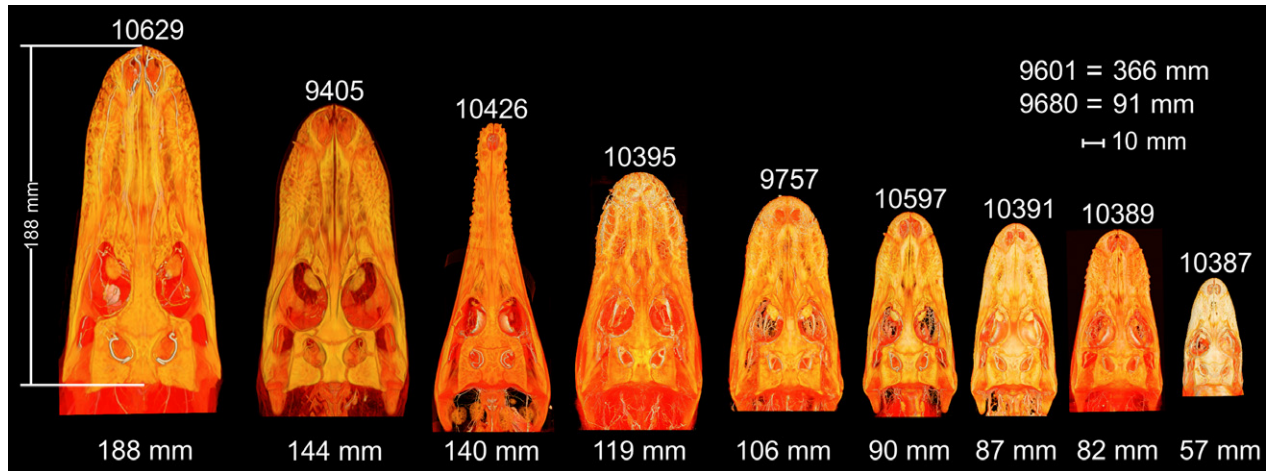

Fig. 1 Volume rendering of one crocodile (OUVC 10426) and eight alligator heads. Specimens are arranged by size, with OUVC accession number above the head and the skull length in mm below. Skulls were measured from the tip of the premaxilla to the dorsal aspect of the supraoccipital. OUVC 9601 and 9680 were not CT-scanned, but were included in this study.
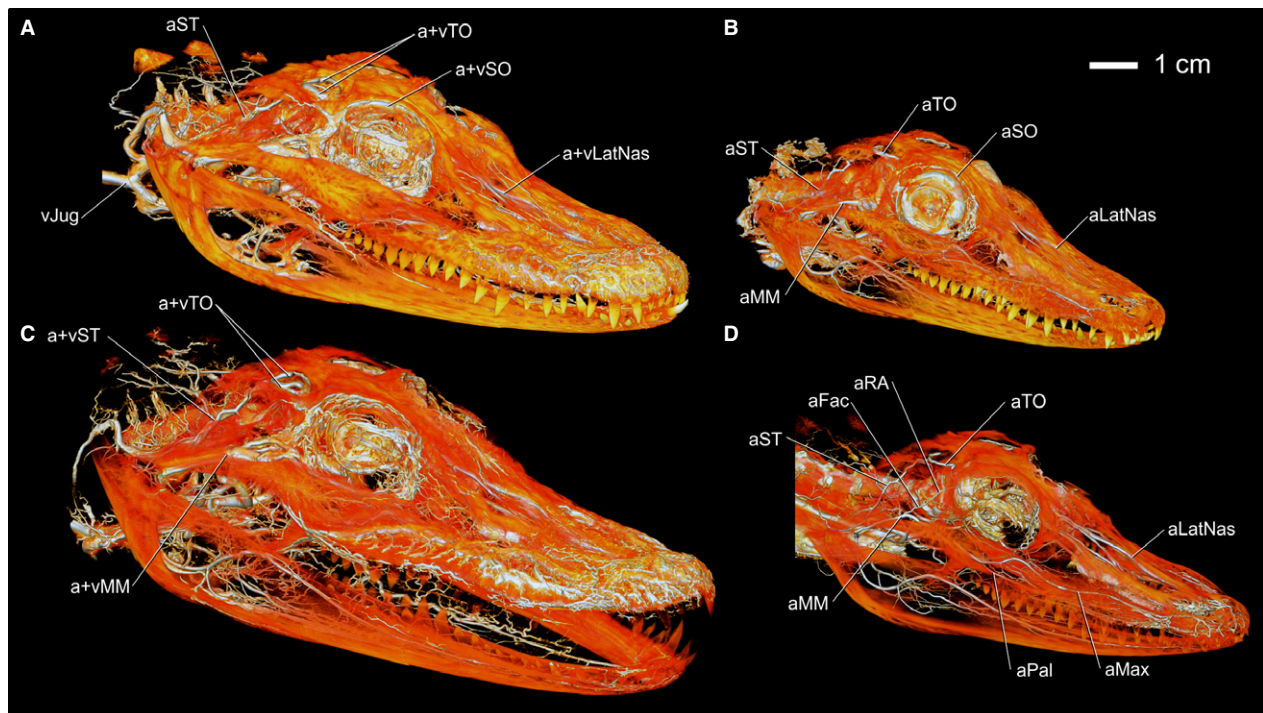

Fig. 2 Volume renderings of four *Alligator mississippiensis* specimens in right rostrodorsolateral view showing blood vessels of the head. (A) OUVC 9757 venous and arterial injection. (B) OUVC 10389 arterial and venous injection. (C) OUVC 10395 arterial and venous injection. (D) OUVC 10597 arterial injection. Vessel names: aFac, facial artery; aLatNas, lateral nasal artery; aMax, maxillary artery; aMM, maxillomandibular artery; aPal, palatine artery; aRA, rostral auricular artery; aSO, supraorbital artery; aST, stapedial artery; aTO, temporoorbital artery; vJug, jugular vein; vLatNas, lateral nasal vein; vMM, maxillomandibular vein; vSO, supraorbital vein; vST, stapedial vein; vTO, temporoorbital vein.

differential-contrast dual-vascular injection (DCDVI) method developed in our lab (e.g. Holliday et al. 2006) and based on our earlier techniques (Sedlmayr & Witmer, 2002).

A post-injection scan (Fig. 3) at the same settings as the first CT scan was acquired to allow the subsequent registration of the skull and soft-tissue anatomy onto the post-injection data. CT datasets are available from the Dryad database (http://dx.doi.org/10.5061/dryad.mt64k). This sequence is necessary because the barium in the latex solution is denser than bone, which introduces some CT artifacts (e.g. beam hardening, streaking) into the data. The blood vessels course close to and within bones, creating a situation where it is nearly impossible to separate the bony and vascular signals, resulting in a skull surface that would be marred by vascular artifacts. This two-step scanning procedure alleviates these issues, resulting in a high-quality hard-tissue (e.g. skull) dataset and a high-quality vascular dataset.

Digital segmentation was completed using Avizo 7 (FEI Visualization Sciences Group, Burlington, MA, USA) on a Dell T3400 Workstation with 8 gbytes of RAM and an nVidia Quadro FX 4600 video card running Microsoft WINDOWS 7 ENTERPRISE. As noted, after data processing and analysis, the segmented tissues from the pre-injection dataset were registered to the post-injection dataset, resulting in an artifact-free skull placed in association with the injected blood vessels. This approach gives the clearest picture of the relationships between the blood vessels and bone such that they can be viewed together, in isolation, with the skull transparent etc. Segmented blood vessels were then imported into MAYA (Autodesk, San Rafael, CA, USA) from Avizo. MAYA was used to overlay 3D surfaces
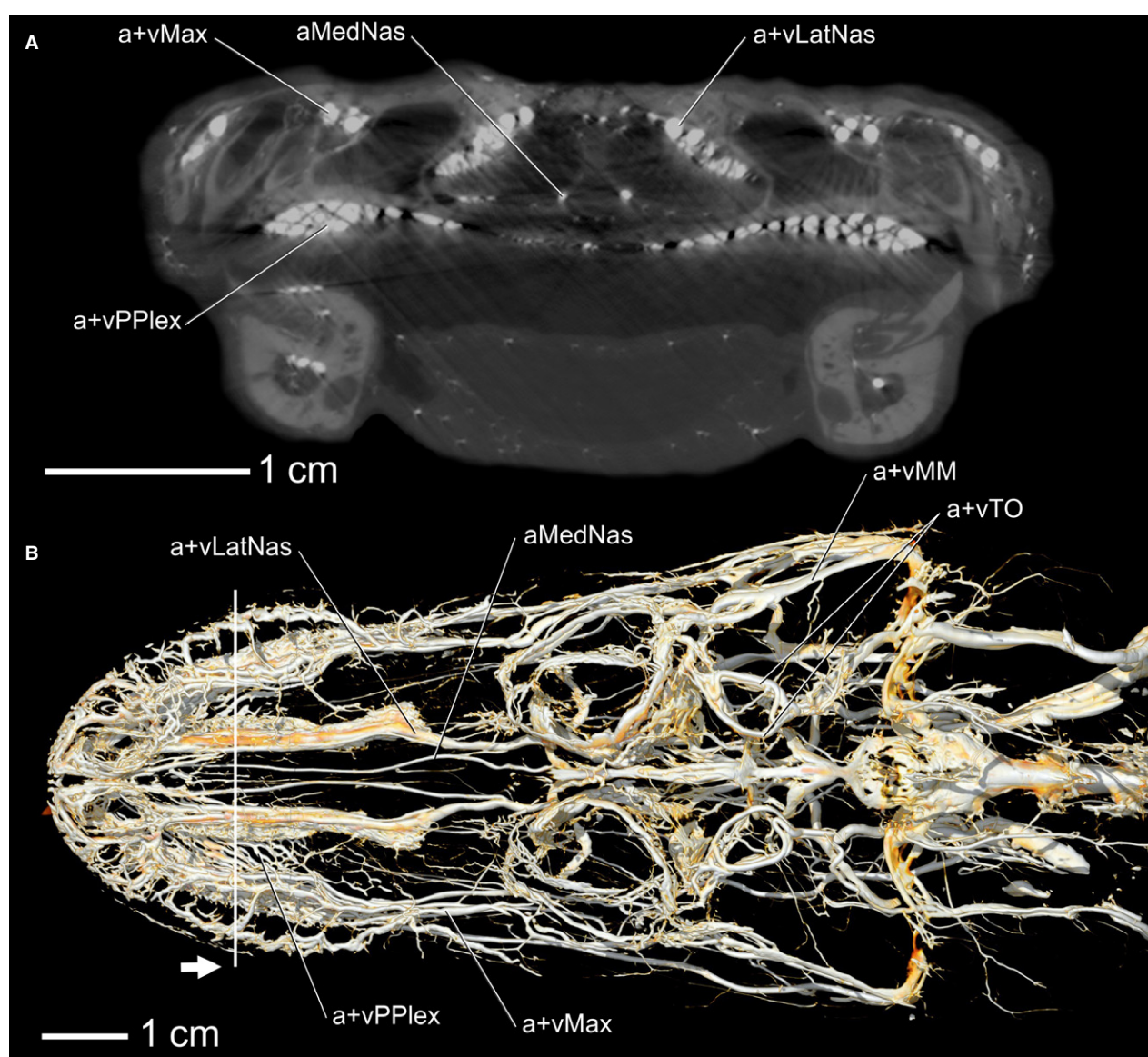

Fig. 3 *Alligator mississippiensis*, OUVC 9757. (A) CT slice of the nasal region showing arteries and veins. (B) Volume rendering of a dorsal view of OUVC 9757 showing arteries and veins. White line indicates the location of the CT slice and the white arrow indicates direction of view. Vessel names: vMax, maxillary vein; aMedNas, medial nasal artery; vLatNas, lateral nasal vein; vPPlex, venous palatal plexus; vMM, maxillomandibular vein; vTO, temporoorbital vein.

representing the blood vessels, using the segmented blood vessels from Avizo as templates. Using this process, the CT datasets from different alligator specimens were composited into a single model within Maya, allowing the strengths of each dataset to be represented and a more complete model generated. The Maya model was then exported as a 3D PDF file (Supporting Information Fig. S1) that represents a diagrammatic illustration yet is interactive and allows the user/reader to manipulate the model and observe finer details. The 3D PDF is considered an intrinsic part of this article, and the reader is encouraged to download and open it alongside the publication. The 3D PDF also contains 'views' of the in-text figures that can then be rotated to examine the figure in a broader context. To access the 3D PDF, open the file and click on the center of the page to activate the 3D function. The model in the 3D PDF can be rotated and zoomed, structures can be rendered transparent or removed, and the name of the blood vessel can be found by clicking on it and looking in the Model Tree on the left side of the page and viewing the highlighted name.

After CT scanning, segmentation, and 3D visualization were complete, specimens were dissected to verify the digital results. Multiple dried skulls of *Alligator mississippiensis*, *Crocodylus johnstoni*, *Crocodylus porosus,* and *Crocodylus novaeguinea* were observed to confirm and record vascular osteological correlates (Witmer, 1995a, b). Many Batson's injections and corrosion casts in the OUVC remaining from Sedlmayr (2002) were observed to compare specimens and supplement the crocodilian sample.

Results

Major vessels of the head that supply and drain sites of thermal exchange

Overview

The major arteries supplying the head are ultimately branches of the common carotid artery. The common carotid artery bifurcates into internal and external carotid arteries. The branches of the internal carotid artery are traced first through the cerebral carotid artery to the brain, then through the stapedial artery through to the orbit. The branches of the external carotid artery are then followed around the quadrate to the rostral aspect of the laterotemporal fenestra. The major veins that drain the head are described in this section, except veins from the mandible, orbital, nasal, and palatal regions. The veins will be described in a caudal to rostral fashion, against the flow of blood, to enhance the comparability of the arteries and veins, as they generally follow each other closely.

Common carotid artery

Similar to birds, the single common carotid artery of crocodilians courses cranially within a median osteomuscular canal, bounded dorsally by vertebrae and ventrally by cervical musculature (Rathke, 1866; Reese, 1914, 1915; Sedlmayr, 2002). Ventral to the first and second cervical vertebrae, the common carotid artery bifurcates into right and left branches which course between m. rectus capitis ventralis pars medialis and pars lateralis (Sedlmayr, 2002). The common carotid artery then courses dorsolaterally to the

basal tuber where it passes caudoventral to the occipital condyle and branches into internal and external carotid arteries (Figs 4–7).

Internal carotid artery

The internal carotid artery branches off from the common carotid artery and almost immediately bifurcates into a large, dorsomedially directed cerebral carotid artery and a dorsally directed stapedial artery (Figs 4 and 8).

Cerebral carotid artery

The cerebral carotid artery enters the carotid canal in the otoccipital bone, where it ultimately passes through the basisphenoid and into the pituitary fossa. Within the pituitary fossa, the cerebral carotid artery branches into the common encephalic and orbital arteries. As reported by Sedlmayr (2002), small sphenopalatine arteries branch off the internal carotid artery before the bifurcation into orbital and common encephalic arteries. The orbital artery passes rostrally into the orbit and supplies the caudal aspect of the orbit and replaces the internal ophthalmic artery during development (Burda, 1969). The common encephalic artery sends off hypophyseal branches, courses dorsally along the lateral wall of the sella turcica, and then bifurcates into rostral and caudal encephalic arteries. Both right and left caudal encephalic arteries course caudomedially across the dorsum sellae and unite with the contralateral artery to form the basilar artery (Fig. 5). The rostral encephalic artery bifurcates into a rostrally directed branch, the rostral cerebral artery, and a caudodorsally directed branch, the caudal cerebral artery. The rostral cerebral artery courses rostrally along the laterosphenoid, gives off the middle cerebral artery laterally, and then courses towards the midline to anastomose with the contralateral rostral cerebral artery (Burda, 1969; Sedlmayr, 2002; Figs 5, 8, and 9).

Stapedial artery

After branching off from the internal carotid artery, the stapedial artery continues to course dorsally just lateral to the foramen magnum, where it gives off the occipital arteries in a caudodorsomedial direction and then turns laterally toward the cranioquadrate canal along the ridge forming the ventral border of the paroccipital process (Sedlmayr, 2002). Upon reaching the caudal aperture of the cranioquadrate canal, the stapedial artery turns dorsally and accepts the anastomosis with the external carotid artery along its ventral surface. The stapedial artery passes rostroventral to the paroccipital process and enters the cranioquadrate canal. The stapedial artery grooves the dorsal aspect of the quadrate, medial to the articulation of the paroccipital process and the squamosal and travels dorsomedially through the cranioquadrate canal, grooving the lateral aspect of the otoccipital and exits the canal into the
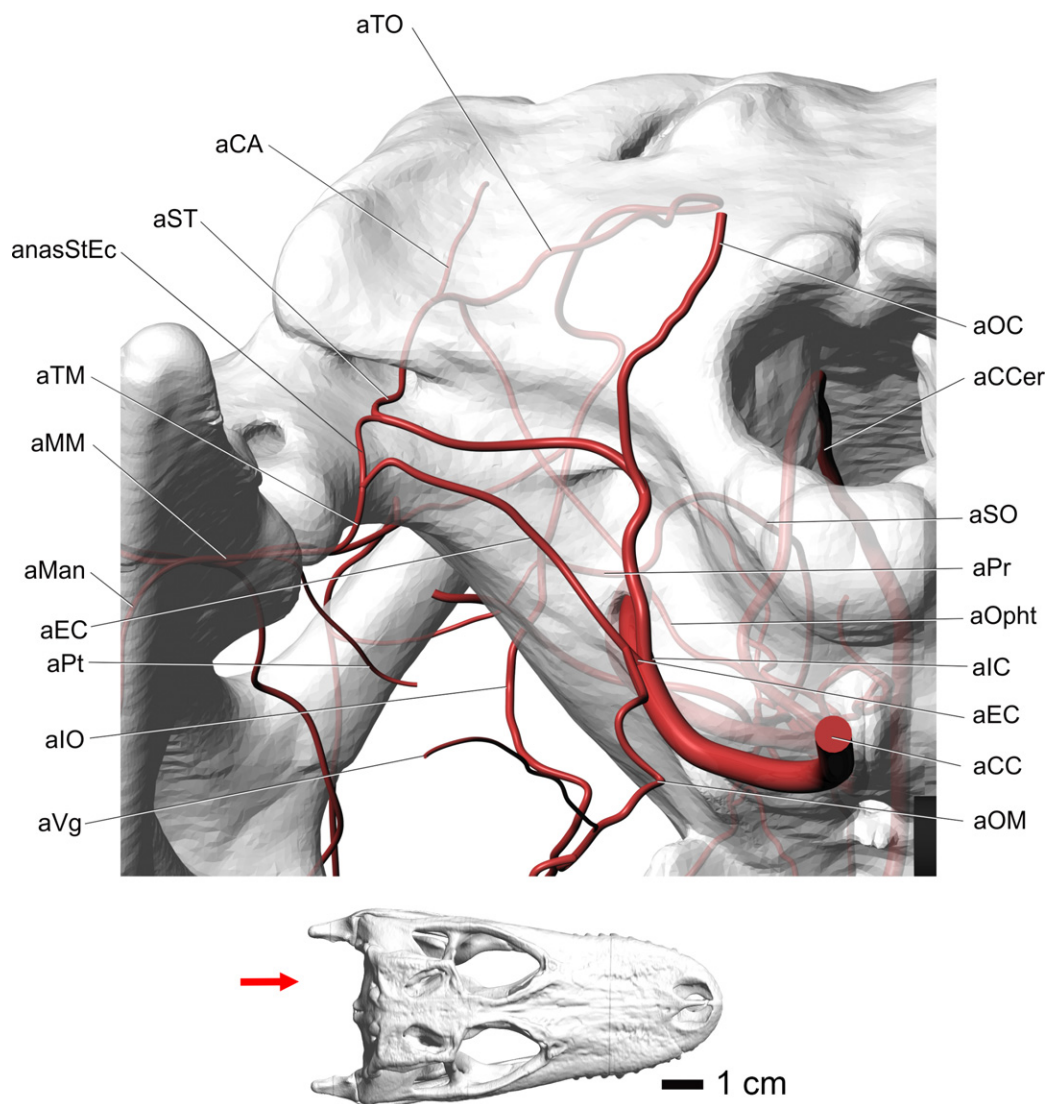
Fig. 4 *Alligator mississippiensis*, caudal view, showing the modeled representations of the major arteries of the head. Skull is semitransparent. Arrow in inset at bottom shows the view in the image above. Vessel names: aTO, temporoorbital artery; aCA, caudal auricular artery; aST, stapedial artery; anasStEc, anastomosis between stapedial artery and external carotid vessels; aTM, temporomandibular artery; aMM, maxillomandibular artery; aMan, mandibular artery; aEC, external carotid artery; aPt, pterygoid artery; aIO, infraorbital artery; aVg, vagus artery; aOC, occipital artery; aCCer, caudal cerebral artery; aSO, supraorbital artery; aPr, profundus artery; aOpht, ophthalmotemporal artery; aIC, internal carotid artery; aCC, common carotid artery; aOM, oromandibular artery.

middle-ear space (Sedlmayr, 2002). Upon entering the middle-ear space, the stapedial artery bifurcates into a dorsal branch, the temporoorbital artery, and a medial branch, the caudal auricular artery (Figs 4 and 6). The caudal auricular artery supplies a mass of erectile tissue and a plexus that ramifies across the ventral aspect of the squamosal (Sedlmayr, 2002; Montefeltro et al. 2016), often leaving a series of grooves and foramina in the squamosal (Figs 2, 4, and 6–8).

Temporoorbital artery
Within the middle-ear space, the temporoorbital artery sends a ventrally directed branch that grooves the

otoccipital and then grooves the prootic in a ventromedial direction, then anastomoses with the internal carotid artery. This artery provides an anastomotic connection, allowing blood to flow between the temporoorbital and internal carotid arteries. The temporoorbital artery courses rostrodorsomedially into the canal located at the articulation between the otoccipital, squamosal, and parietal. The artery then exits the canal through its external foramen onto the dorsal aspect of the dorsotemporal fossa. The temporoorbital artery then forms an oddly consistent, medially directed hairpin loop (Figs 7 and 9) along the caudodorsal aspect of m. adductor mandibulae externus profundus, then turns laterally to course along the lateral aspect of the
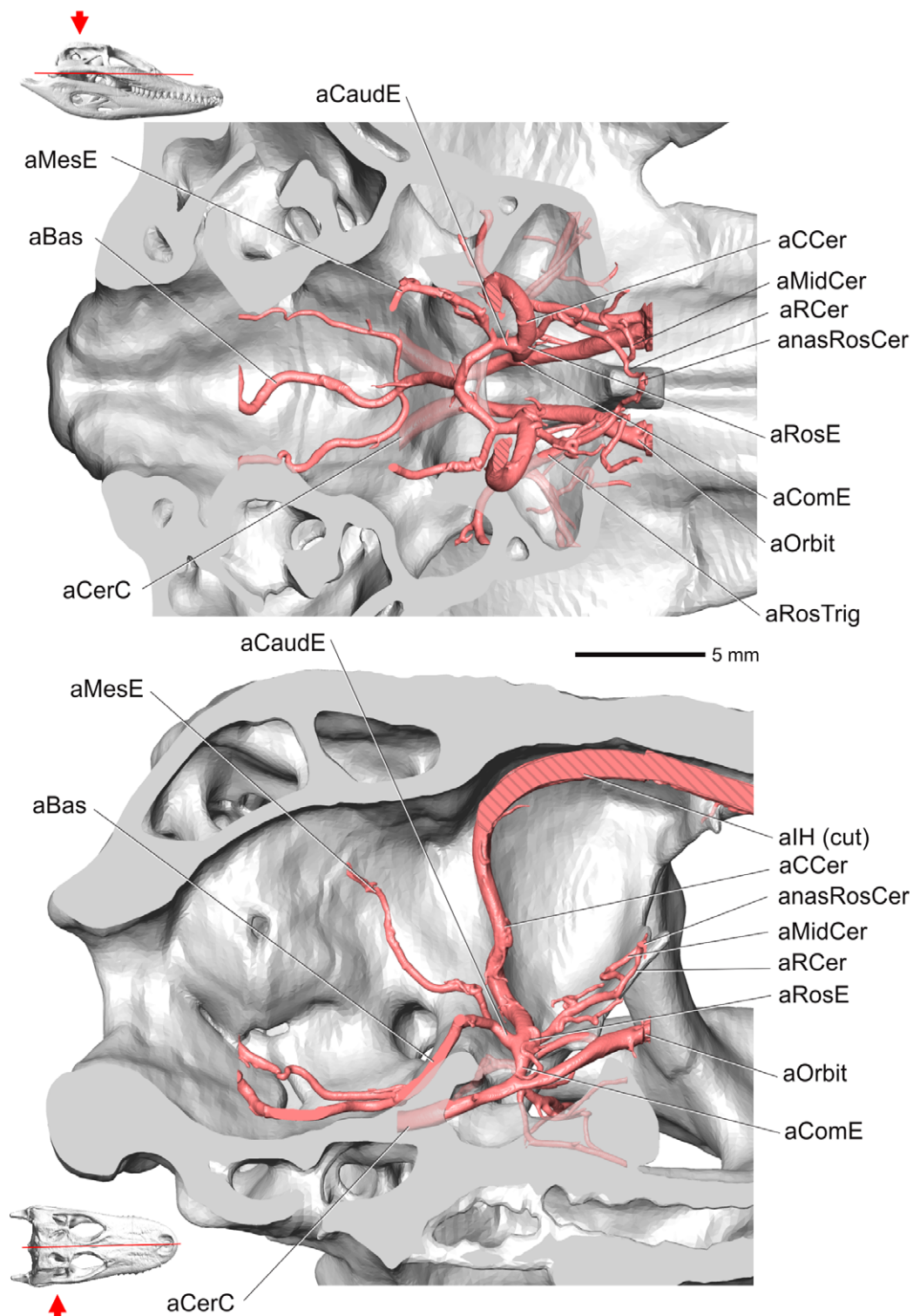
Fig. 5 *Alligator mississippiensis*, OUVC 10395. Top, dorsal view showing the encephalic arteries. Hatching patterns represent cut arteries. Bottom, medial view showing the encephalic arteries. Inset with red line indicates the plane of section and the arrow indicates view. Vessel names: aCaudE, caudal encephalic artery; aMesE, mesencephalic artery; aBas, basilar artery; aCerC, cerebral carotid artery; aCCer, caudal cerebral artery; aMidCer, middle cerebral artery; aRCer, rostral cerebral artery; anasRosCer, anastomosis between rostral cerebral vessels; aRosE, rostral encephalic artery; aComE, common encephalic artery; aOrbit, orbital artery; aRosTrig, rostral branch of trigeminal artery; aIH, interhemispheric artery.
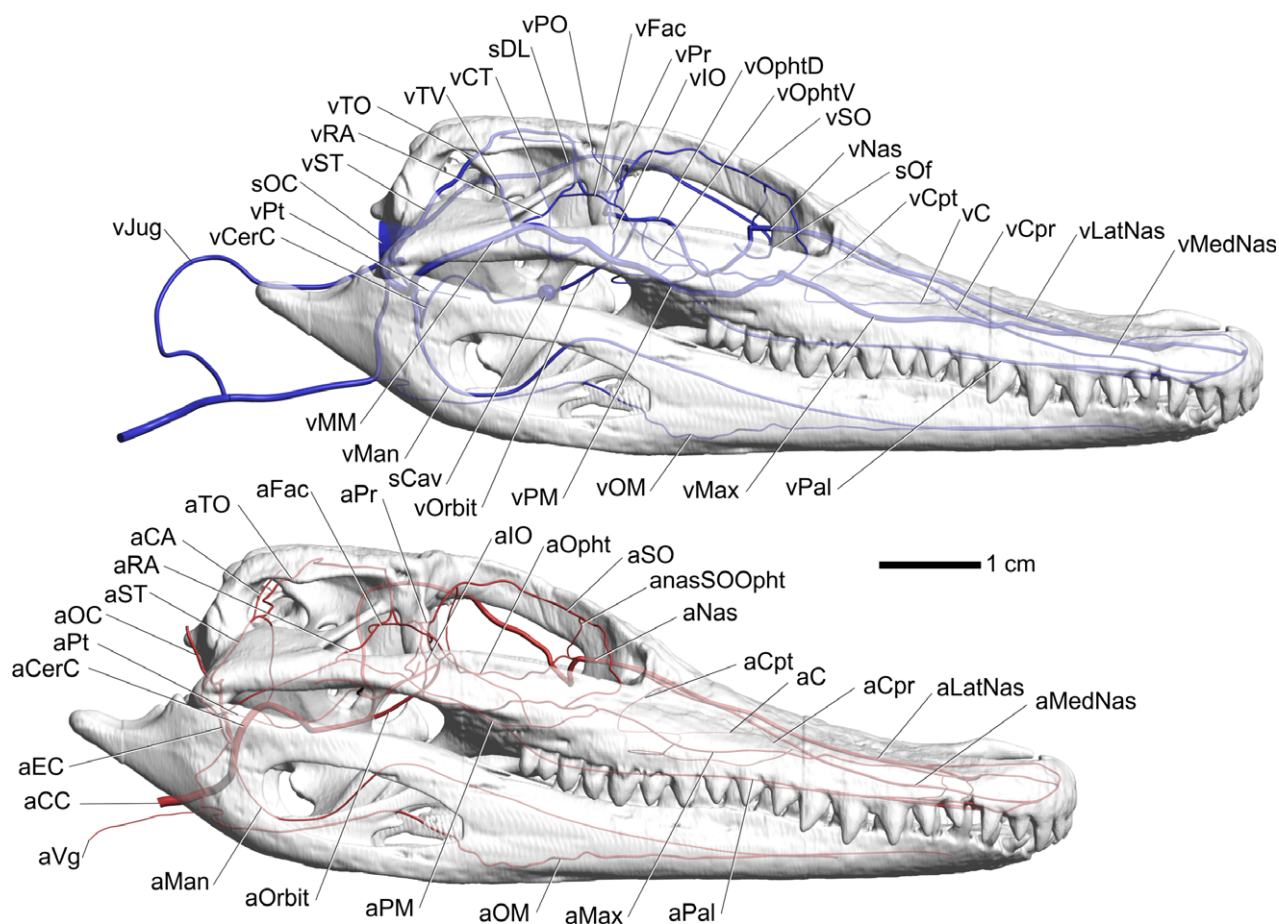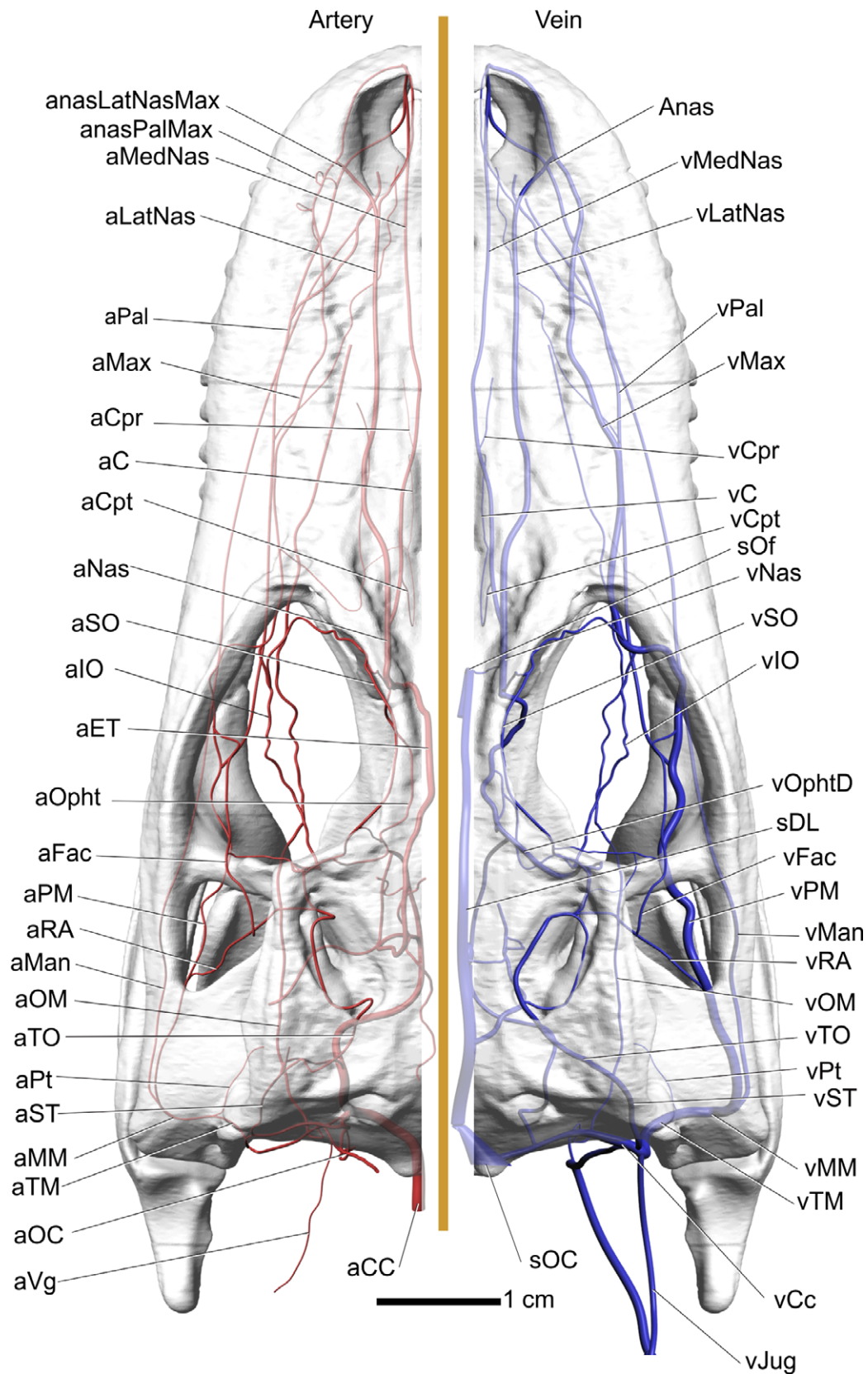
Fig. 6 *Alligator mississippiensis*, right lateral view. Top, modeled representations of the cephalic veins. Bottom, modeled representations of the cephalic arteries. Skull is semitransparent. Vessel names: vPO, postorbital vein; sDL, dorsal longitudinal sinus; vCT, cerebrotectal vein; vTV, transverse sinus; vTO, temporoorbital vein; vRA, rostral auricular vein; vST, stapedial vein; sOC, occipital sinus; vPt, pterygoid vein; vCerC, cerebral carotid vein; vJug, jugular vein; vFac, facial vein; vPr, profundus vein; vIO, infraorbital vein; vOphtd, dorsal branch of ophthalmotemporal vein; vOphtv, ventral branch of ophthalmotemporal vein; vSO, supraorbital vein; vNas, common nasal vein; sOf, olfactory sinus; vCpt, postconchal vein; vC, conchal vein; vCpr, preconchal vein; vLatNas, lateral nasal vein; vMedNas, medial nasal vein; vMM, maxillomandibular vein; vMan, mandibular vein; sCav, cavernous sinus; vOrbit, orbital vein; vPM, palatomaxillary vein; vOM, oromandibular vein; vMax, maxillary vein; vPal, palatine vein; aFac, facial artery; aTO, temporoorbital artery; aCA, caudal auricular artery; aRA, rostral auricular artery; aST, stapedial artery; aOC, occipital artery; aPt, pterygoid artery; aCerC, cerebral carotid artery; aEC, external carotid artery; aCC, common carotid artery; aVg, vagus artery; aMan, mandibular artery; aOrbit, orbital artery; aPM, palatomaxillary artery; aOM, oromandibular artery; aMax, maxillary artery; aPal, palatine artery; aMedNas, medial nasal artery; aLatNas, lateral nasal artery; aCpr, preconchal artery; aC, conchal artery; aCpt, postconchal artery; aNas, common nasal artery; anasSOOpht, anastomosis between supraorbital and ophthalmotemporal vessels; aSO, supraorbital artery; aOpht, ophthalmotemporal artery; aIO, infraorbital artery; aPr, profundus artery.

Fig. 7 *Alligator mississippiensis*, top view. Left, modeled representations of the cephalic arteries. Right, modeled representations of the cephalic veins. Skull is semitransparent. Vessel names: anasLatNasMax, anastomosis between lateral nasal and maxillary vessels; anasPalMax, anastomosis between palatine and maxillary vessels; aMedNas, medial nasal artery; aLatNas, lateral nasal artery; aPal, palatine artery; aMax, maxillary artery; aCpr, preconchal artery; aC, conchal artery; aCpt, postconchal artery; aNas, common nasal artery; aSO, supraorbital artery; aIO, infraorbital artery; aET, ethmoid artery; aOpht, ophthalmotemporal artery; aFac, facial artery; aPM, palatomaxillary artery; aRA, rostral auricular artery; aMan, mandibular artery; aOM, oromandibular artery; aTO, temporoorbital artery; aPt, pterygoid artery; aST, stapedial artery; aMM, maxillomandibular artery; aTM, temporomandibular artery; aOC, occipital artery; aVg, vagus artery; aCC, common carotid artery; sOC, occipital sinus; Anas, anastomosis; vMedNas, medial nasal vein; vLatNas, lateral nasal vein; vPal, palatine vein; vMax, maxillary vein; vCpr, preconchal vein; vC, conchal vein; vCpt, postconchal vein; sOf, olfactory sinus; vJug, jugular vein; vCc, caudal head vein; vTM, temporomandibular vein; vMM, maxillomandibular vein; vST, stapedial vein; vPt, pterygoid vein; vTO, temporoorbital vein; vOM, oromandibular vein; vRA, rostral auricular vein; vMan, mandibular vein; vPM, palatomaxillary vein; vFac, facial vein; sDL, dorsal longitudinal sinus; vOphtd, dorsal branch of ophthalmotemporal vein; vIO, infraorbital vein; vSO, supraorbital vein; vNas, common nasal vein.
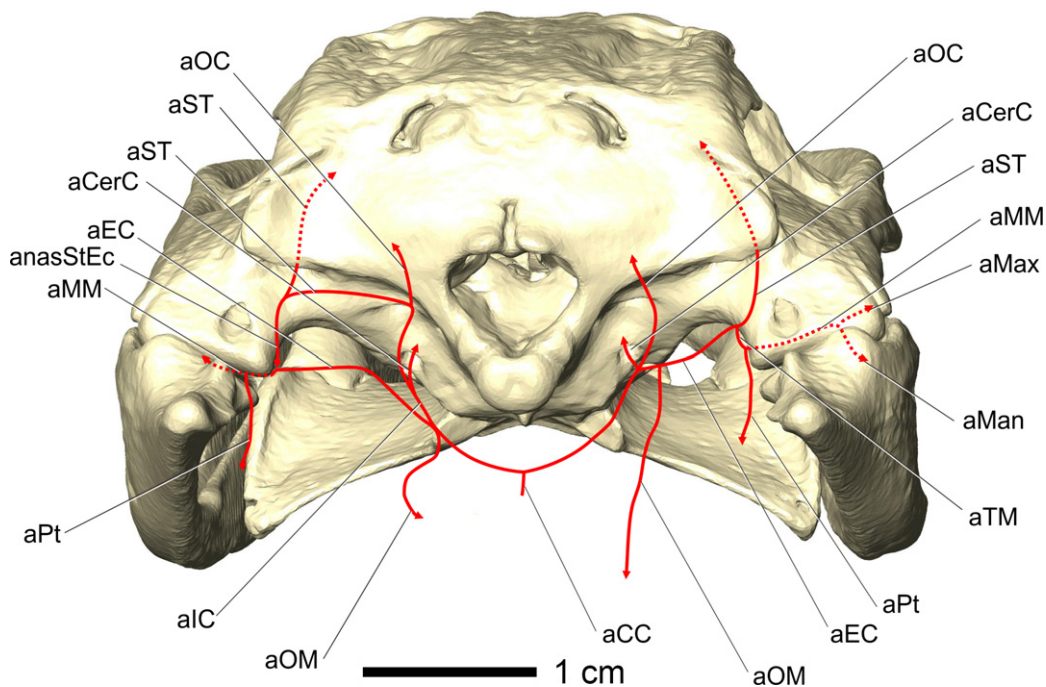
Artery

Vein

anasLatNasMax
anasPalMax
aMedNas
aLatNas
aPal
aMax
aCpr
aC
aCpt
aNas
aSO
aIO
aET
aOpht
aFac
aPM
aRA
aMan
aOM
aTO
aPt
aST
aMM
aTM
aOC
aVg
aCC

Anas
vMedNas
vLatNas
vPal
vMax
vCpr
vC
vCpt
sOf
vNas
vSO
vIO
vOphtD
sDL
vFac
vPM
vMan
vRA
vOM
vTO
vPt
vST
vMM
vTM
sOC
vCc
vJug

1 cm

Fig. 8 *Alligator mississippiensis*, OUVC 10597. Caudal view of an alligator showing a diagram of the vascular variations in the caudal region of the head. Variations were present on the right side, whereas the left side had the more typical diapsid pattern. Vessel names: aCC, common carotid artery; aCerC, cerebral carotid artery; aEC, external carotid artery; aIC, internal carotid artery; aMan, mandibular artery; aMax, maxillary artery; aMM, maxillomandibular artery; anasStEc, anastomosis between stapedial artery and external carotid vessels; aOC, occipital artery; aOM, oromandibular artery; aPt, pterygoid artery; aST, stapedial artery; aTM, temporomandibular artery.

dorsotemporal fossa. At the rostral extent of the dorsotemporal fossa and the caudal aspect of the postorbital bone, the temporoorbital artery gives off the lateral postorbital artery laterally. The temporoorbital artery then turns ventrally to pass through the temporal canal along the rostromedial aspect of m. adductor mandibulae externus profundus. Medial to the postorbital and capitate process of the laterosphenoid (Fig. 9), the artery forms a small rete mirabile. Both the temporoorbital artery and vein send vessels into a small, loose plexus which appears to be an avian-like ophthalmic rete, or possibly represents an ancestral precursor (Sedlmayr, 2002). In OUVC 9680, a juvenile alligator from Sedlmayr's (2002) study, a small rete composed of very fine vessels was observed as rostrally directed braches from the temporoorbital artery. The small size of the observed rete could be due to the age of the specimen. Further evidence is being collected to better elucidate this structure. Rostral to the rete, the temporoorbital artery turns medially and gives off the profundus artery medially and the infraorbital artery ventrally. The profundus artery branches into the supraorbital and ophthalmotemporal arteries within the orbital region, rostral to the laterosphenoid (Figs 6 and 9). A variable branching pattern of the infraorbital artery was found either medial or lateral to the supraorbital artery or sharing a large anastomotic connection with the orbital artery that looks as if it was branching from the orbital artery (Figs 2, 4, and 6–9).

External carotid artery

The branches of the external carotid artery demonstrated a considerable amount of variation between specimens and even between right and left sides of the same specimen, which makes a consistent branching pattern difficult to describe. Nevertheless, a clearly diapsid branching pattern is detectable (Fig. 8). The external carotid artery branches from the common carotid artery along the lateral border of m. rectus capitis ventralis, just ventrolateral to the foramen magnum, and is a dorsolaterally directed artery. The external carotid artery passes along the lateral aspect of m. rectus capitis ventralis and the medial aspect of m. pterygoideus dorsalis. The external carotid artery then continues dorsolaterally across the dorsal attachment of m. pterygoideus dorsalis into the internal mandibular process (Holliday et al. 2013). Along the medial aspect of the quadrate, the external carotid artery bifurcates into the ventrally directed temporomandibular artery and a dorsally directed branch that anastomoses with the stapedial artery. This anastomotic branch is likely the homolog of the mandibular artery branching off from the stapedial artery, which was shifted laterally onto the external carotid artery during the developmental reorganization of the skull that is characteristic of crocodilians (e.g. rotation and flattening, lateral spread of the quadrates, suturing of pterygoid and quadrate to braincase; Figs 4, 6, and 8).
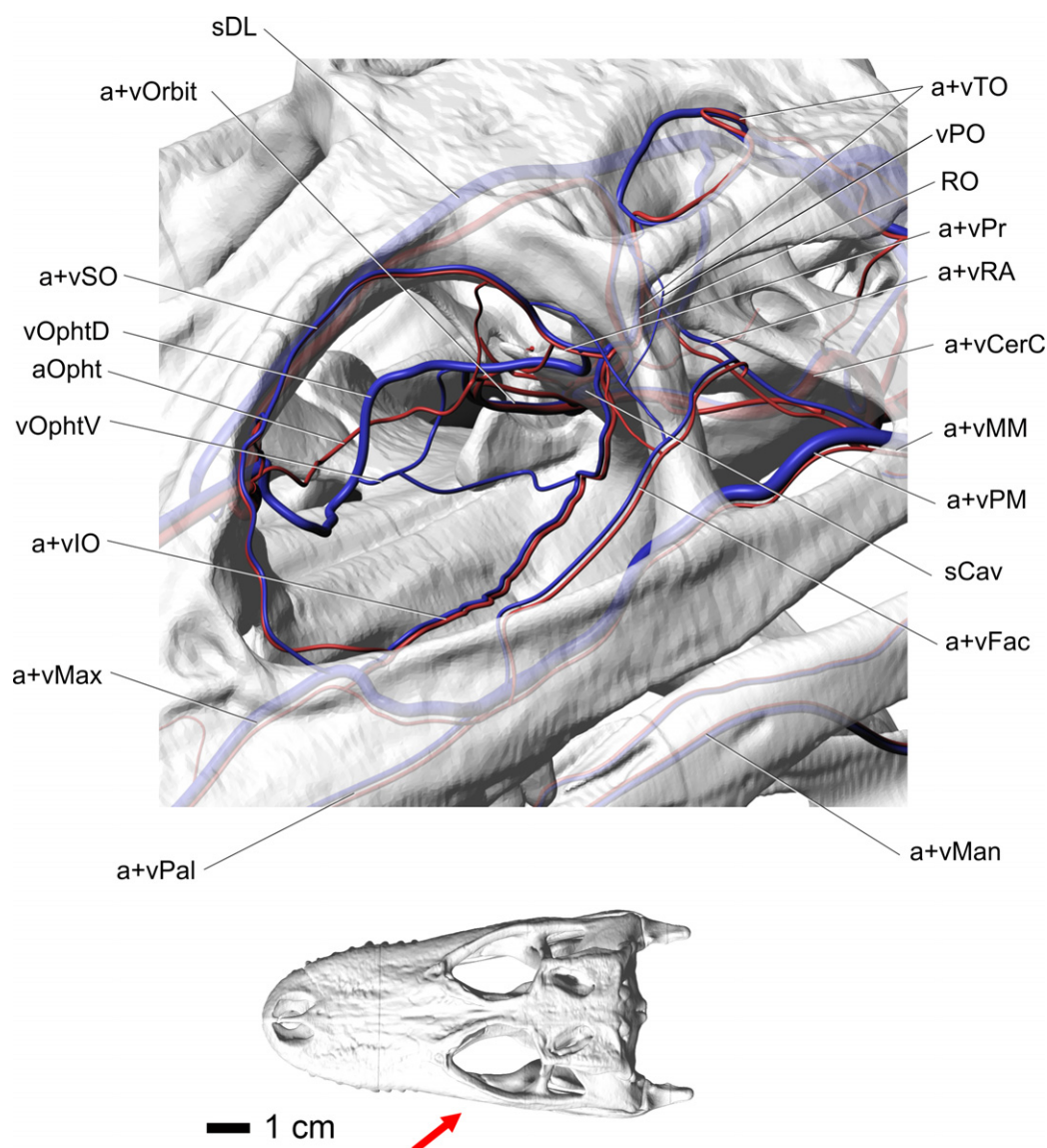
Fig. 9 *Alligator mississippiensis,* rostrolateral oblique view of the blood vessels of the orbital region. Skull is semitransparent. Arrow in inset indicates orientation and view. Vessel names: sDL, dorsal longitudinal sinus; vOrbit, orbital vein; vSO, supraorbital vein; vOphtd, dorsal branch of ophthalmotemporal vein; aOpht, ophthalmotemporal artery; vOphtv, ventral branch of ophthalmotemporal vein; vIO, infraorbital vein; vMax, maxillary vein; vPal, palatine vein; vMan, mandibular vein; vFac, facial vein; sCav, cavernous sinus; vPM, palatomaxillary vein; vMM, maxillomandibular vein; vCerC, cerebral carotid vein; vRA, rostral auricular vein; vPr, profundus vein; RO, ophthalmic rete; vPO, postorbital vein; vTO, temporoorbital vein.

Temporomandibular artery

After continuing from the external carotid artery, the temporomandibular artery courses ventrolaterally to the ventromedial aspect of the quadrate (Fig. 7) and across the ventral aspect of the m. depressor mandibulae, then over the dorsal surface of m. pterygoideus dorsalis (Sedlmayr, 2002). The temporomandibular artery then courses around the medial aspect of the quadrate to pass rostral to the mandibular process of the quadrate, where it branches into the pterygoid and maxillomandibular arteries (Figs 2–4 and 7). The pterygoid artery passes rostromedially and then ramifies to supply the m. pterygoideus ventralis and dorsalis (Sedlmayr, 2002). The maxillomandibular artery continues to course laterally along the rostroventral aspect of the quadrate (Figs 4 and 6–8).

Oromandibular artery

The oromandibular artery, as noted above, was found to have a number of variations in its branching pattern. This artery can branch from either the external or common carotid arteries (Fig. 8) but here it will be considered a branch of the external carotid artery. After branching from the external carotid artery, the oromandibular artery courses ventrally along the lateral side of the m. rectus capitis ventralis and splits along the medial side of m. pterygoideus ventralis into rostral and caudal branches (Sedlmayr, 2002).

The rostral branch courses rostrally with the glossopharyngeal nerve to the esophagus and the caudal branch, the vagus artery, courses with the vagus nerve (Sedlmayr, 2002; Figs 4 and 6–8).

Maxillomandibular artery

The maxillomandibular artery courses along the rostrolateral aspect of the quadrate and then the ventral aspect of the quadratojugal-jugal articulation (Figs 7 and 9) and curves around the caudal border of m. adductor mandibulae externus superficialis on the lateral aspect of the muscle (Holliday et al. 2013). The artery then courses rostrally along the ventromedial aspect of the jugal. Medial to the postorbital process of the jugal, the maxillomandibular artery gives off the facial artery, is renamed the palatomaxillary artery, and then curves around the medial aspect of the jugal and onto the dorsal surface of the ectopterygoid bone and enters the orbital region (Fig. 7). The facial artery in this study was found to be variable or in some cases absent (Figs 2, 4, 6, and 7–9).

Variation

A specimen of *A. mississippiensis* (OUVC 10597) showed a substantial deviation from the pattern presented in Fig. 8. On the right side of the specimen, the stapedial artery, which normally courses ventral to the ridge on the paroccipital process, was not present. The occipital artery branched off near the cerebral carotid in the place of the stapedial artery. The stapedial artery instead branched off directly from the external carotid artery, in the place of the anastomotic branch. The temporomandibular artery was unaffected. The left side of the specimen was found to be consistent with the commonly observed branching pattern described above. Despite the major deviation in branching pattern on the right side, the branches ultimately reached their usual destinations, highlighting the consistency of blood vessels and their osteological correlates.

Most of the veins of the caudal portion of the head travel with the artery of the same name and demonstrate a surprisingly consistent pattern. Because of this close positioning, the veins will be described from caudal to rostral, against the flow of venous blood, to enhance comparability between the descriptions of the arteries and veins.

Caudal head vein

The occipital sinus has a lateral extension which passes between the first cervical vertebra and the otoccipital that anastomoses with veins draining the head. This condition is similar to the iguanian caudal head vein (but not necessarily all squamates, as this condition is variable in squamates), which anastomoses with the lateral head vein before forming the internal jugular vein (Oelrich, 1956). The caudal head vein was described by Hopson (1979) in crocodilians. The caudal head vein travels laterally across the dorsal aspect of the otoccipital fossa and caudoventral to the external carotid artery along the ventral border of the quadrate (Hopson, 1979). This connection between the caudal head vein and the temporomandibular vein would allow a pathway for blood to enter or exit the spinal veins (Fig. 10).

Stapedial vein

The stapedial vein drains the temporoorbital veins and middle-ear space. The stapedial vein exits the cranioquadrate canal caudally and courses ventrally across the paroccipital process where, along the medial articular condyle of the quadrate, the caudal head vein accepts the stapedial vein. The stapedial vein travels through the cranioquadrate canal with the stapedial artery and then courses through the middle-ear space and traverses the dorsotemporal canal to enter the dorsotemporal fossa, where it receives the medial and lateral temporoorbital veins. The venous-injected specimens examined did not form the same hairpin loop as the temporoorbital artery (Fig. 7). The medial and lateral tributaries, the temporoorbital veins, curve around each respective aspect of the dorsotemporal fossa and anastomose with each other along the rostral aspect of the dorsotemporal fossa. The temporoorbital veins receive the postorbital veins within the dorsotemporal fossa after the postorbital veins traverse the postorbital canal in the rostrolateral aspect of the dorsotemporal fossa. The postorbital veins pass laterally through the postorbital bone to anastomose with the veins of the postorbital plexus (Figs 2, 6, 7, and 10).

Temporomandibular vein

The temporomandibular vein is formed by the union of the maxillomandibular and pterygoid veins (Sedlmayr, 2002) and courses medially from the rostroventral aspect of the quadrate and joins the caudal head vein to form the jugular vein. The oromandibular vein joins the caudal head vein and temporomandibular veins and contributes to the jugular vein (Reese, 1914). This pattern would potentially give cooled venous blood a pathway into the spinal veins or into the jugular vein. The jugular vein then courses caudally along the ventrolateral aspect of the m. rectus capitis lateralis (Figs 7 and 10).

Maxillomandibular vein

The maxillomandibular vein courses adjacent to the maxillomandibular artery, passing ventral to the quadrate and quadratojugal and then lateral to the m. adductor mandibulae externus superficialis and across the ventral aspect of the laterotemporal fenestra. The maxillomandibular vein then receives the large rostral auricular veins that ramify into the postorbital plexus. The veins of the postorbital plexus then pass lateral to the postorbital bone and anastomose with the postorbital veins to form the large postorbital plexus in the caudolateral aspect of the orbit. The postorbital plexus receives tributaries from the postorbital, supraorbital, and dorsal palpebral veins (Figs 2, 7, and 10).
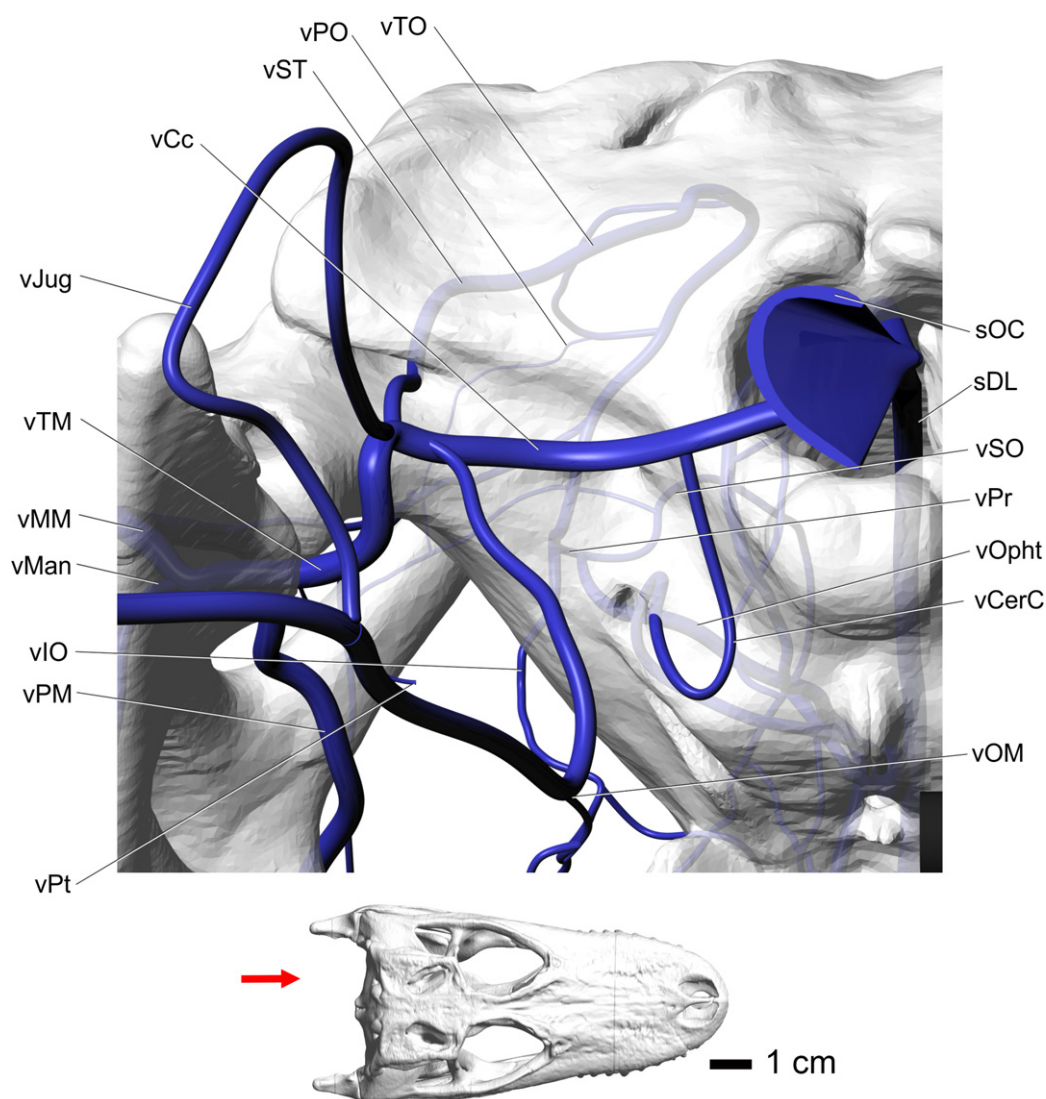
Fig. 10 *Alligator mississippiensis*, caudal view, showing the modeled representations of the major veins of the head. Skull is semitransparent. Arrow in the inset indicates orientation and view. Vessel names: sDL, dorsal longitudinal sinus; vSO, supraorbital vein; vOphtv, ventral branch of ophthalmotemporal vein; vIO, infraorbital vein; vMan, mandibular vein; vPM, palatomaxillary vein; vMM, maxillomandibular vein; vCerC, cerebral carotid vein; vPr, profundus vein; vPO, postorbital vein; vTO, temporoorbital vein; vST, stapedial vein; vCc, caudal head vein; vJug, jugular vein; vTM, temporomandibular vein; vPt, pterygoid vein; vOM, oromandibular vein; sOC, occipital sinus.

The *C. johnsoni* specimen (OUVC 10426) showed little variation from the patterns described above. The only notable difference was the diameter of the medial and lateral temporoorbital veins in the dorsotemporal fenestra, where the lateral branch was much smaller than the medial. This condition was not observed in the alligators sampled, where the medial and lateral veins were of similar diameters.

Orbital region

Overview
The arteries and veins of the orbital region course in close apposition. The temporoorbital artery is the parent artery of the infraorbital, supraorbital, and ophthalmotemporal arteries which supply most of the tissues in the orbit. The venous drainage of the orbit is via the temporoorbital veins, but some blood can drain into the cavernous sinus.

Temporoorbital artery
The temporoorbital artery enters the orbital region by passing caudomedial to the capitate process of the laterosphenoid and then passes medially along the rostral aspect of the laterosphenoid. The temporoorbital artery then branches into the dorsomedially directed profundus artery and the ventrolaterally directed infraorbital artery (Sedlmayr, 2002). The profundus artery courses medially along the rostral aspect of the laterosphenoid, where it branches

into the supraorbital and ophthalmotemporal arteries (Fig. 9).

Supraorbital artery
The supraorbital artery branches from the profundus artery, similar to the avian condition. The supraorbital artery also shows anastomotic connections with the postorbital plexus, similar to galliform birds (e.g. turkeys, pheasants, and chickens). After branching off from the profundus artery, the supraorbital artery courses across the suture between the laterosphenoid and frontal bones, then across the ventro-lateral aspect of the frontal, following a tortuous course. Similar to birds (Porter & Witmer, 2016), the supraorbital artery sends branches ventrally that anastomose with the ophthalmotemporal artery. As the supraorbital artery courses along the ventrolateral aspect of the frontal, it sends small branches that create faint grooves in the ventro-lateral aspect of the frontal and sends nutrient arteries into the frontal. These grooves provide osteological evidence for the course of the supraorbital artery through the orbit. In the rostrodorsal aspect of the orbit, the supraorbital artery anastomoses with the ophthalmotemporal artery, sending branches to supply the Harderian gland. The supraorbital artery then courses along the frontal to the frontal/pre-frontal suture, where the vessel splits into dorsal and ventral branches. The dorsal branch courses towards the postnasal fenestra found between the frontal and pre-frontal. Along with the ophthalmic nerve, the dorsal branch of the supraorbital artery passes rostrally into the nasal region, where it anastomoses with the ethmoid artery. The ventral branch of the supraorbital artery passes across the lateral aspect of the lacrimal duct and anastomoses with the maxillary artery. This artery often sends an anastomotic branch to the infraorbital artery before it anastomoses with the maxillary artery (Figs 2, 6, 7, and 9).

Ophthalmotemporal artery
After branching from the profundus artery, the ophthal-motemporal artery courses along the rostral aspect of the laterosphenoid, then passes medial to the eyeball and dor-sal to the optic nerve. The ophthalmotemporal artery then anastomoses with the orbital artery (Burda, 1969; Sedlmayr, 2002). The ophthalmotemporal artery then curves rostrally along the medial portion of the orbit. The ophthalmotem-poral artery then courses rostrodorsally to anastomose with the supraorbital artery to supply the nasal region and Harderian gland (Figs 6, 7, and 9).

Infraorbital artery
The infraorbital artery courses rostrolaterally around the ventrolateral aspect of the eyeball and dorsal to m. tensor periorbitae. Within the rostroventrolateral aspect of the orbit, ventral to the lacrimal and maxilla articulation, the artery anastomoses with the maxillary artery. A similar con-dition was found in *Iguana iguana*, where the infraorbital

artery forms the maxillary artery when it entered the max-illa (Porter & Witmer, 2015). In crocodilians, the maxillary artery is a separate branch of the external carotid artery yet still demonstrates this anastomosis with the infraorbital artery. A similar anastomotic connection has not been demonstrated in birds. The branching of the infraorbital artery from the temporoorbital artery was variable. The infraorbital artery was found to branch in the pattern described by Sedlmayr (2002) but was also found to branch medial to the supraorbital artery in many specimens. In one alligator specimen (OUVC 10597), the infraorbital artery appears to branch from the anastomosis between the oph-thalmotemporal and orbital arteries (Figs 6, 7, and 9).

Orbital artery
The orbital artery is the continuation of the internal carotid artery after the branching off of the encephalic and spheno-palatine arteries from the cerebral carotid artery (Fig. 5). This artery continues rostrally into the orbit through a notch in the rostroventromedial margin of the laterosphenoid and dorsal aspect of the basisphenoid rostrum. Within the orbit, the orbital artery sends numerous anastomotic branches to the ophthalmotemporal artery caudodorsal to the origin of the m. rectus ventralis (Sedlmayr, 2002). This artery supplies most of the caudal aspect of the orbit and takes over the territory of the internal ophthalmic artery (Burda, 1969). During early development, the internal ophthalmic artery passes through the optic foramen and supplies the orbital contents, but it is replaced by the orbital artery through ontogeny and is not present in the orbital region of adults (Burda, 1969; Sedlmayr, 2002; Figs 5, 6, and 9).

Temporoorbital vein
The temporoorbital vein courses along the capitate process of the laterosphenoid and enters the orbital region with the temporoorbital artery, where the vein forks to receive the profundus vein dorsally and the infraorbital vein ven-trally. Similar to the temporoorbital artery, the vein turns medially and travels across the suture of the frontal and laterosphenoid, where it branches into the ophthalmotem-poral rostromedially and the supraorbital vein dorsally (Figs 2, 6, 7, 9, and 10).

Ophthalmotemporal vein
The ophthalmotemporal vein receives a dorsal and ventral branch (Fig. 9) just caudal to the m. rectus lateralis. The dor-sal branch passes along the lateral aspect of m. retractor bulbi and then along the ventral surface of m. rectus dor-salis. The ophthalmotemporal vein passes between the ven-tral and lateral rectus muscles, ventral to the optic nerve. Along the medial aspect of m. retractor bulbi, the ophthal-motemporal vein anastomoses with the supraorbital vein, similar to the artery. The ophthalmotemporal vein then sends branches into the ocular plexiform ring (Sedlmayr, 2002), creating a complex branching pattern medial to the

eyeball, encircling the optic nerve and the surfaces of the rectus muscles facing the optic nerve (Sedlmayr, 2002). The ocular plexiform ring is formed by branches between the supraorbital and ophthalmotemporal vessels and supplies the soft tissues of the orbit. Rostral to the eyeball, the dorsal branch anastomoses with the supraorbital vein and passes into the postnasal fenestra and then into the nasal region. The ventral branch of the ophthalmotemporal vein diverges from the ophthalmotemporal artery near the lateral aspect of m. rectus lateralis, where it then courses rostrally just ventral to the muscle. The vein then courses ventral to the m. rectus ventralis and dorsal to m. tensor periorbitae. The ophthalmotemporal vein passes medial to the Harderian gland, where it receives numerous large tributaries draining the gland. The vein then curves dorsally along the caudal aspect of the prefrontal bone. At the caudal aspect of the postnasal fenestra, the ophthalmotemporal vein accepts the supraorbital and dorsal palpebral veins to form the nasal vein. The nasal vein then continues through the postnasal fenestra into the nasal region (Figs 6, 7, and 9).

Supraorbital vein

The supraorbital vein parallels the supraorbital artery along its tortuous course along the lateral aspect of the frontal bone, where it anastomoses with the frontal, ophthalmotemporal, and palpebral veins. The supraorbital vein anastomoses with the ophthalmotemporal vein yet does not completely participate in the formation of the profundus vein as it does in birds. The supraorbital vein joins with the dorsal palpebral vein and sends caudally directed veins that are tributaries of the temporoorbital vein, but also has a large drainage component through the postorbital plexus to the palatomaxillary vein. Therefore, in crocodilians, the supraorbital has a variable participation in the formation of the profundus and temporoorbital veins and a variable contribution to the small ophthalmic rete (Figs 2, 6, 7, and 9).

Infraorbital vein

The infraorbital vein branches from the temporoorbital vein and courses rostrolaterally, dorsal to m. tensor periorbitae, and ventral to the eyeball. Similar to the infraorbital artery, the vein anastomoses with the maxillary vein in the rostroventral corner of the orbit (Figs 6, 7, and 9).

Orbital vein

The orbital vein drains the venous component of the ocular plexiform ring and the extrinsic eye muscles (Sedlmayr, 2002). The orbital vein courses with the orbital artery and drains into the cavernous sinus through the optic foramen. This pathway may allow blood cooled in the orbital region to enter the dural sinus system and influence at least the temperature of the pituitary gland and hypothalamus (Fig. 9).

Cavernous sinus

The cavernous sinus resides within the pituitary fossa and receives the orbital vein, along with the veins traveling with the cranial nerves (Sedlmayr, 2002) from within the orbit (e.g. abducent and oculomotor veins). The cavernous sinus has anastomotic connections to the trigeminal veins and caudoventral cerebral vein (Sedlmayr, 2002). The cavernous sinus then coalesces into the cerebral carotid veins, to enter the cerebral carotid canal with the cerebral carotid arteries (Figs 6 and 9).

The *C. johnsoni* specimen (OUVC 10426) showed little variation from the patterns described above. The most notable difference was the size of the ophthalmotemporal veins, which were much expanded bilaterally in the specimen examined, which could be attributed to an artifact of the injection process, although the supraorbital veins were not markedly distended.

Nasal region

Overview

The nasal region is a highly vascularized region in the crocodilian head. Of the three named conchal structures, the rostralmost two, the preconcha and concha, are well vascularized and are positioned in the main airflow through the nasal region (Bourke et al. 2014). There are vast submucosal plexuses along the rostral and ventral nasal region that further enhance the vascularization. The nasal region is supplied by the ethmoid artery, a terminal artery from the encephalic region, which branches into the lateral and medial nasal arteries, which are external and internal, respectively, to the cartilaginous nasal capsule. There are anastomotic connections with the maxillary artery that supply additional blood to the nasal region. The venous drainage of the nasal region follows the arteries closely and again will generally be described in a caudal-to-rostral direction to enhance comparability with the description of the arteries. In the postnasal fenestra, the nasal vein, which accepts both the medial and lateral nasal veins, bifurcates into veins that are tributaries to both the dural venous sinuses and the orbital veins, providing direct pathways to neurosensory tissues of the brain and eyes.

The vasculature of the nasal region showed little variation between specimens and closely matched Sedlmayr's (2002) descriptions of this region. This section will focus on broader vascular patterns, osteological correlates, and anastomotic connections and pathways that may have an influence on the temperature of neurosensory tissues.

Ethmoid artery

The ethmoid artery provides the majority of the blood supply to the nasal cavity, with support from anastomotic connections with the maxillary, ophthalmotemporal, and supraorbital arteries. The ethmoid artery is a branch of the rostral encephalic artery, via the caudal cerebral artery,

(Burda, 1969; Sedlmayr, 2002; Almeida & Campos, 2011). The caudal cerebral artery courses dorsally between the cerebrum and optic lobe (Fig. 5), just medial to the tentorial crest and ventral to the cerebrotectal sinus. Within the central sulcus, the right and left caudal cerebral arteries become the interhemispheric arteries and then merge into a single ethmoid artery (Burda, 1969; Sedlmayr, 2002; Almeida & Campos, 2011) which travels rostrally, just ventral to the dorsal longitudinal sinus. In birds, the rostral cerebral artery gives off the cerebroethmoid artery (Baumel, 1993). The cerebroethmoid artery becomes the ethmoid artery (after giving off the rostral cerebral artery) that exits into the orbital region through the ethmoid foramen located just ventral to the olfactory tract. In adult alligators, the interhemispheric branches off of the caudal cerebral artery form the ethmoid artery. During development, the caudal cerebral artery forms an anastomosis with the rostral cerebral artery and when the section of the rostral cerebral artery that would have formed the ethmoid arteries obliterates, the ethmoid arteries are supplied by the larger caudal cerebral arteries (Burda, 1969). The crocodilian ethmoid artery passes ventrally between the olfactory tracts as a single median vessel but still remains dorsal to the septal cartilage and cartilaginous nasal capsule. Caudal to the olfactory bulbs (Fig. 11), the ethmoid artery splits into right and left arteries that turn laterally to curve around the rostrolateral aspect of the olfactory bulbs. Each ethmoid artery then sends branches rostrally that supply the olfactory bulbs, which then pass rostrally to anastomose with the medial nasal artery proper. Burda (1969) called these branches the medial nasal arteries, but we regard the medial/lateral dichotomy as taking place more rostrally. Each ethmoid artery then turns rostrally along the ventrolateral aspect of olfactory bulbs and anastomoses with the supraorbital artery within the postnasal fenestra. Rostral to this anastomosis, the nasal artery traverses the postnasal fenestra and enters the nasal region. The nasal vessels create a groove along the medial border of the prefrontal pillar. Rostral to the prefrontal bone, the nasal artery splits into medial and lateral nasal arteries which then supply the nasal region (Figs 7 and 11).

Medial nasal artery
The medial nasal artery enters the caudodorsal aspect of the cartilaginous nasal capsule through the foramen advehens and courses along the dorsolateral aspect of the nasal septum. The medial nasal artery gives off three small arteries, the postconchal, conchal, and preconchal arteries, which supply each respective conchal structure. The preconcha is the most vascularized of the conchae and the postconcha is the least. The conchal and preconchal arteries anastomose with a branch from the maxillary artery that arises just before the maxillary artery enters the dorsal alveolar canal, and then travels medially, dorsal to the palatine

bone and parallel to the rostral border of the suborbital fenestra (Fig 11). The dorsal part of the anastomotic branch from the maxillary artery contributes to the submucosal plexus on the concha and the ventral part courses to supply the submucosal plexus on the preconcha. The branching pattern and distribution of this anastomotic branch from the maxillary artery are similar to that of the anastomotic branch between the maxillary and sphenopalatine arteries in iguanas (Porter & Witmer, 2015), although in crocodilians this artery does not pass through a foramen in the palatine bone. Branches from the preconchal artery supply a submucosal plexus found dorsal to the rostral aspect of the vomer and along the nasal septum and solum nasi and into the nasal vestibule. This plexus creates a highly vascular mucosal region extending from the nasal vestibule to the primary choana that is in direct contact with air passing through the main nasal cavity on its way to the nasopharyngeal duct. The medial nasal artery courses ventrally along the angle formed by the nasal septum and the solum nasi (Fig. 3) and sends branches laterally into the submucosal plexus that continues within the solum nasi from the preconcha. The medial nasal artery then enters the premaxilla through canals on the caudal aspect of the bone and along the rostral aspect of the nasal vestibule, and anastomoses with the arteries within the premaxilla derived from the maxillary, palatine, and lateral nasal arteries (Figs 3, 6, 7, and 11).

Lateral nasal artery
After branching from the nasal artery, the lateral nasal artery exits the nasal capsule through the foramen epiphaniale to pass along the caudodorsal aspect of the nasal cartridges with the lateral nasal branch of the ophthalmic nerve (Witmer, 1995b; Sedlmayr, 2002). The lateral nasal artery then courses rostrally dorsal to the tectum nasi and ventral to the nasal bones, sending branches into the bone through numerous foramina (Fig. 12). The lateral nasal artery then supplies a vast vascular network within the nasal gland. Rostral to the nasal gland, the lateral nasal artery ramifies into multiple arteries that surround the lateral nasal nerve and courses rostrally into the nasal vestibule. The lateral nasal artery then sends branches laterally to the premaxilla/maxilla suture to the medial subnarial foramen to anastomose with the maxillary artery (Figs 7 and 11). Rostral to this anastomosis, the lateral nasal artery branches into the erectile arteries of the nasal vestibule (Sedlmayr, 2002; Figs 2, 3, 6, 7, and 11).

Lateral nasal vein
The lateral nasal veins drain the tissue of the narial fossa along the caudal aspect of the nasal vestibule. The maxillary vein sends a branch through the medial subnarial foramen that anastomoses with the lateral nasal vein. The lateral nasal vein courses caudally with the lateral nasal artery and nerve. The lateral nasal vein drains the nasal gland and
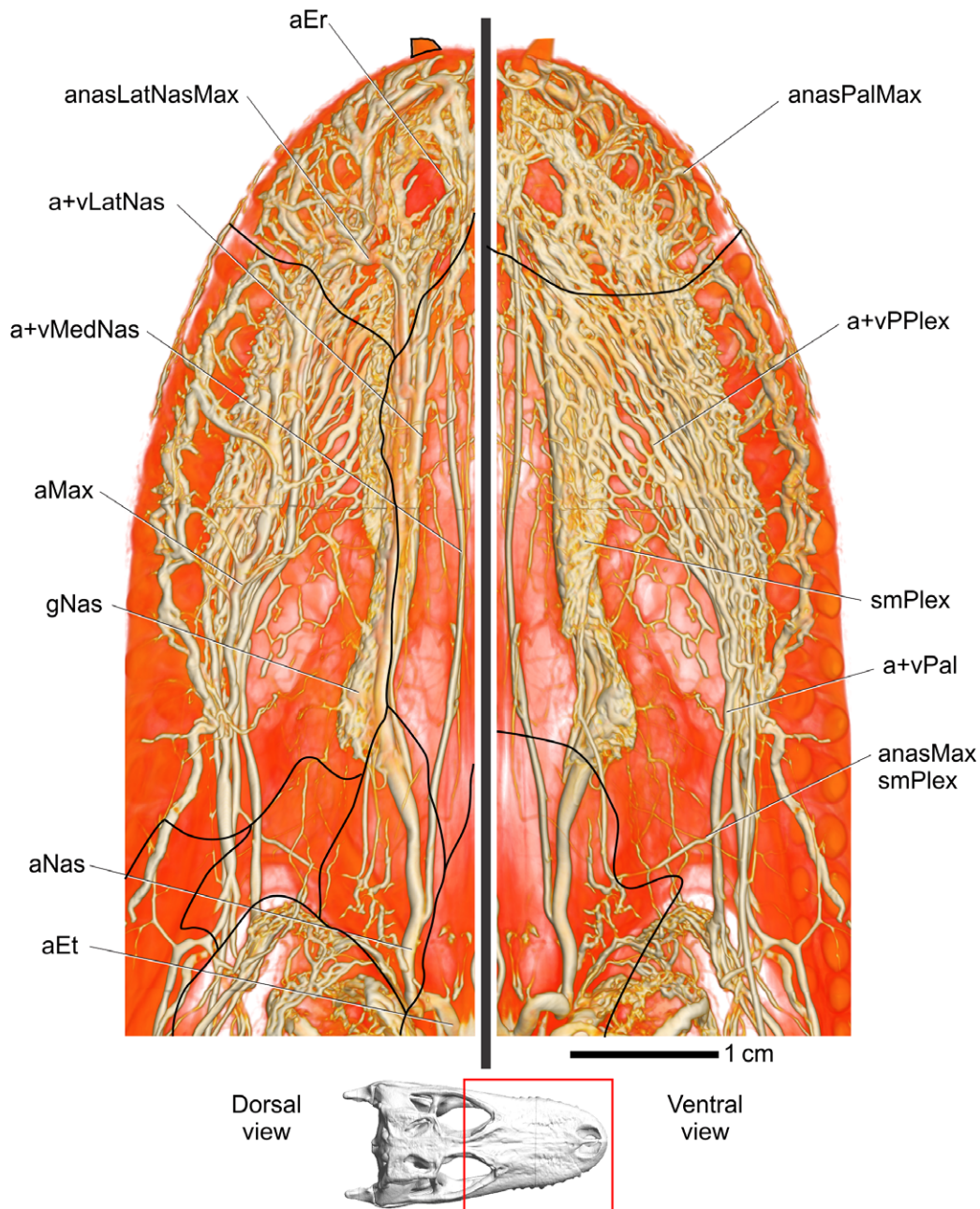
Fig. 11 *Alligator mississippiensis*, OUVC 9757. Volume rendering of both the nasal region in dorsal view (left) and palatal region in ventral view (right), indicating the extensive vascularization of these regions. Inset indicates area region. Black lines indicate the approximate location of sutures. Vessel names: aEr, erectile arteries; anasLatNasMax, anastomosis between lateral nasal and maxillary vessels; vLatNas, lateral nasal vein; vMedNas, medial nasal vein; aMax, maxillary artery; gNas, nasal gland; aNas, common nasal artery; aET, ethmoid artery; anasMaxsmPlex, anastomosis between maxillary artery and submucosal plexus; vPal, palatine vein; smPlex, submucosa plexus on ventral part of airway; vPPlex, venous palatal plexus; anasPalMax, anastomosis between palatine and maxillary vessels.

vascular plexus of the preconcha, drains the highly vascular nasolacrimal duct, and then accepts the medial nasal vein to become the nasal vein (Figs 2, 3, 6, 7, and 11).

Medial nasal vein
The medial nasal vein courses along the nasal septum with the medial nasal artery and nerve. The vein drains the submucosal plexus along the solum nasi and the plexus medial to the preconcha. The medial nasal vein then courses to the ventrolateral aspect of the olfactory bulb, where it sends small branches into the dorsal longitudinal sinus, delivering cooled blood directly to the dural sinus system. Again, the medial and lateral nasal veins then join to form the nasal vein (Figs 2, 5, 7, and 11).
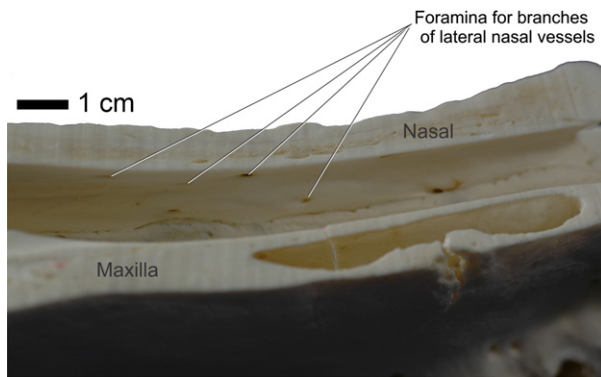
Foramina for branches
of lateral nasal vessels

1 cm

Nasal

Maxilla

Fig. 12 *Alligator mississippiensis,* OUVC 9601. Medial view of left side of sagittally sectioned skull demonstrating the foramina housing branches of the lateral nasal vessels and nerves.

Nasal vein

Within the postnasal fenestra, the nasal vein is formed by the union of the medial and lateral nasal veins. The nasal vein then sends a branch that anastomoses with the olfactory sinus and the dorsal longitudinal sinus. This vein is a large branch along the ventral aspect of the olfactory bulb, ventral to the ethmoid arteries, which would allow more cooled blood to enter the dural sinus system. The vein then travels caudally through the postnasal fenestra into the orbital region. The nasal vein then accepts the supraorbital vein and creates a large venous plexus or sinus. The dorsal longitudinal sinus drains the nasal region, which allows blood cooled there to pass in close proximity to neural tissue. Likewise, blood from the nasal region may then flow into the orbit and ophthalmotemporal veins to pass over tissues associated with the eyeball. These two vascular routes would allow crocodilians to control the temperature of neurosensory tissues using a well vascularized region of the head (Figs 6, 7, and 11).

The *C. johnsoni* specimen (OUVC 10426) showed little variation from the patterns described above. The vasculature of the nasal region was more elongate, obviously to accommodate the longirostrine condition of *C. johnsoni*.

Oral region

Overview

The oral region is the only crocodilian site of thermal exchange that has received some attention from physiologists (Spotila et al. 1977; Smith, 1979). The oral mucosa of the palate demonstrates a large plexus, the palatal plexus, which comprises both arteries and veins from the palatine vessels. The maxillary and palatine vessels show numerous anastomotic connections, indicating there is likely an exchange of blood between the maxillary and palatine vessels. These anastomotic connections are also shared with the nasal region within the narial fossa, indicating potential pathways from the oral region to the nasal region. The

arteries are described in the opposite direction of blood flow, from caudal to rostral and because of the similarity in branching patterns, the veins are described in this caudal-to-rostral direction as well.

Palatomaxillary artery

The palatomaxillary artery is the continuation of the maxillomandibular artery after the branching of the facial artery in the ventral aspect of the laterotemporal fenestra. The palatomaxillary artery passes along the rostrolateral aspect of the m. adductor mandibulae externus superficialis aponeurosis (Sedlmayr, 2002). The palatomaxillary artery then passes medial to the ventral process of the postorbital bone and enters the ventral aspect of the orbital region. It gives off jugal branches, the rostral and caudal internal jugal arteries, which enter the medial aspect of the jugal bone through foramina located along the rostral and caudal aspect of the postorbital process of the jugal, respectively. The palatomaxillary artery then courses through the ventral aspect of the orbital region just dorsal to the suture between the ectopterygoid and the maxilla (Fig. 9). Along the rostral aspect of the suture, the palatomaxillary artery branches into the rostrally directed maxillary artery and the rostroventrally directed palatine artery (Reese, 1914; Figs 6, 7, and 9).

Maxillary artery

As the maxillary artery passes dorsal to the ectopterygoid-maxilla suture, it anastomoses with both the infraorbital and supraorbital arteries. The maxillary artery sends a caudomedially directed branch that courses along the dorsal aspect of the palate (Fig. 11). As noted above, the artery passes dorsal to the lamina of the palatine bone that roofs the nasopharyngeal duct (Witmer, 1995b). The artery then turns rostrally along the lateral aspect of the vomer and nasal septum and anastomoses with the medial nasal artery to supply the submucosal plexus located along the nasal septum and ventral airway. This artery also sends branches that supply the plexus found on the preconcha. The maxillary artery then travels rostrally and enters the dorsal alveolar canal. Within the maxilla, a large portion of the medial wall of the dorsal alveolar canal is eroded by the antorbital sinus, allowing the sinus and the maxillary neurovascular bundle to come into contact. The maxillary artery sends a branch that supplies a plexus over the antorbital sinus (Sedlmayr, 2002). Along its course through the maxilla, the maxillary artery sends branches ventrally that anastomose with the palatine artery. These branches themselves send branches laterally into a rostrolaterally directed canal that is found lateral to the tooth row, supplying it and the lateral aspect of the skull and skin. These canals and vessels are not always continuous and extend throughout the lateral aspect of the maxilla, but may span three to four teeth. At the maxilla-premaxilla suture, the maxillary artery sends branches through the medial subnarial foramen that

anastomoses with the lateral nasal artery. Another anastomotic branch courses through the ventral subnarial foramen to anastomose with the palatine artery (Sedlmayr, 2002), forming the palatonasal anastomosis. No nerves were detected on a gross anatomical level passing through the medial subnarial foramen. After the anastomosis with the lateral nasal artery, the maxillary artery (Figs 7 and 11) continues rostrally as the subnarial artery, which enters the premaxilla and passes through canals on the rostral aspect of the nasal vestibule to anastomose with the erectile arteries, which supply the cavernous tissue that aids nostril closure (Bellairs & Shute, 1953; Martin & Bellairs, 1977; Figs 2, 3, 6, 7, 9, and 11).

Palatine artery

After branching from the palatomaxillary artery along the rostral border of the suborbital fenestra, the palatine artery courses rostrally, ventral to the maxilla and medial to the tooth row, just ventral to a longitudinal row of foramina. The palatine artery sends branches into these foramina, often deeply grooving them. These branches course through the alveolus and anastomose with the maxillary artery. In skeletal preparations, the alveolus is deeply grooved, offering some osteological evidence for the blood supply to the tooth socket. Near the caudal aspect of the maxilla, the palatine artery ramifies (Fig. 11) to form the palatal plexus (Sedlmayr, 2002). These branches course rostromedially and quickly anastomose with other branches to create a large plexus that spans the ventral surface of the entire bony secondary palate. Rostrally, the palatine artery sends branches that pass through foramina in the maxilla and premaxilla to anastomose with the maxillary artery (Fig. 6). As noted above, just caudal to the maxilla-premaxilla suture, the palatine artery sends an anastomotic branch through the ventral subnarial foramen that anastomoses with the maxillary and lateral nasal arteries, forming the palatonasal anastomosis. The palatine artery then courses rostrally to enter canals in the premaxilla, where it anastomoses with the medial and lateral nasal arterie, as well as the maxillary artery (Figs 3, 6, 7, 9, and 11).

Palatomaxillary vein

The palatomaxillary vein courses with the palatomaxillary artery, accepting tributaries in a pattern similar to that of the arterial branches. After the branching of the rostral auricular vein into the postorbital plexus, the palatomaxillary vein passes medial to the postorbital process of the jugal and then dorsal to the ectopterygoid, where it runs next to the maxillary nerve. Along the rostral aspect of the ectopterygoid, the palatomaxillary veins bifurcate into the dorsally directed maxillary vein, and the ventral directed palatine vein, which passes ventrally through the suborbital foramen to pass ventrally along the maxilla (Figs 6, 7, 9, and 10).

Maxillary vein

The maxillary vein courses through the infraorbital space with the maxillary artery and enters the maxilla through the dorsal alveolar foramen located in the ventrolateral aspect of the bone. As the maxillary vein courses through the maxilla, it is in close apposition with branches of the maxillary artery. Rostrally, the maxillary vein receives an anastomotic tributary from the lateral nasal veins through the medial subnarial foramen. The maxillary vein has an anastomosis with the facial vein, which ultimately anastomoses with the ethmoid veins, providing a pathway for blood from the maxillary and palatine veins to reach the dorsal longitudinal sinus (Figs 6, 7, 9, and 11).

Palatine vein

The palatine vein is a tributary of the palatomaxillary vein and courses with the palatine artery. The palatine vein courses along the lateral border of the suborbital fenestra, lateral to m. pterygoideus dorsalis and enters the palatal mucosa. Ventral to the palatal shelf of the maxilla, the palatine vein accepts ventrally directed branches through the longitudinal row of foramina that anastomose with the maxillary veins. Just rostral to the suborbital fenestra, the palatine veins ramify along with the arteries and form the palatal plexus. The palatine veins send numerous branches medially that anastomose with the contralateral veins along the ventral aspect of the bony palate, greatly increasing the surface area for thermal exchange and cooling blood along the dorsal aspect of the oral region. Rostrally, the palatine vein accepts a tributary through the ventral subnarial foramen that anastomoses with the maxillary vein and ultimately the lateral nasal vein. Along the ventral aspect of the premaxilla, the palatine veins pass dorsally through canals to anastomose with the medial and lateral nasal veins and erectile veins (Figs 6, 7, 9, and 13).

Palatopharyngeal vein

The palatopharyngeal vein is a tributary of the maxillary vein and ramifies across the ectopterygoid and pterygoid bone, anastomosing with the palatine veins medially. Ventral to the palatine bones, a vast plexus is formed across the entire dorsal surface of the oral region, from the premaxilla to the choana (Fig. 13).

Sublingual vein

In a similar condition to that in squamates (Porter & Witmer, 2015), the veins of the ventral oral region – the lingual, sublingual, and intramandibular veins – drain into the maxillomandibular (via the intramandibular), or jugular (via the oromandibular) veins. This creates a situation where essentially all of the cooled blood from the ventral oral region bypasses pathways to neurosensory tissues and drains directly to the jugular vein and ultimately the heart. The only exception to this was the mandibular vein that sends branches into the pterygoid plexus (Fig. 13), which has
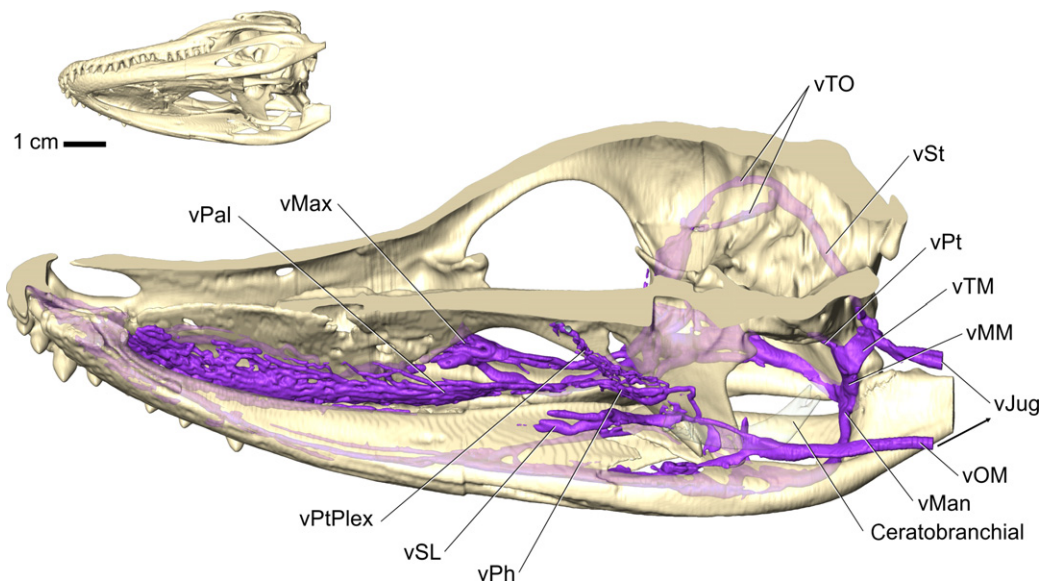
Fig. 13 *Alligator mississippiensis*, OUVC 10387. Right ventrolateral view of sagittally sectioned skull demonstrating the veins of the tongue. Perfusion into the distal aspects of the tongue was not sufficient, yet the veins draining the tongue are present. Blood from the ventral head drains into the jugular vein, bypassing neurosensory tissues like the brain and eyes. Vessel names: vTO, temporoorbital vein; vST, stapedial vein; vPt, pterygoid vein; vTM, temporomandibular vein; vMM, maxillomandibular vein; vJug, jugular vein; vMax, maxillary vein; vPal, palatine vein; vPtPlex, pterygoid plexus; vSL, sublingual vein; vPh, palatopharyngeal vein; vMan, mandibular vein; vOM, oromandibular vein.

anastomotic connections with the trigeminal veins and potentially the dural sinuses (Fig. 13).

The *C. johnsoni* specimen (OUVC 10426) showed little variation from the patterns described above. The palatal plexus was found to be more elongate than that found in the alligator specimens yet was still highly plexiform. The dorsal alveolar canal (and maxillary neurovasculature contained within) was positioned more dorsally than in alligators and even was dorsal to the nasal passage caudal to the nasal vestibule. This more dorsal positioning of the maxillary vessels resulted in longer anastomotic connections with the palatine vessels than those found in alligators.

Discussion

Crocodilians are a highly apomorphic group yet show conserved vascular patterns that have, to a limited degree, been tested for involvement in thermoregulatory processes. Physiological processes such as heart rate hysteresis and shunting blood to either the periphery or core have received the most attention (Smith, 1976, 1979; Drane et al. 1977; Smith et al. 1978; Franklin & Seebacher, 2003; Seebacher & Franklin, 2004, 2007). Unfortunately, selective head or brain cooling has not been tested in crocodilians as it has been in mammals, birds, and squamates, although the findings presented here suggest that such studies are warranted. A number of vascular patterns have been shown to be important in other reptiles, such as the nasal veins in squamates that shunt blood directly into the dural sinuses, having a direct influence on brain temperature (Crawford, 1972). A lack of data on the blood vessels involved in

physiological thermoregulation in crocodilians has left a gap in the understanding of the whole-body and selective brain cooling abilities in crocodilians.

The orbital region of crocodilians is well vascularized, which is consistent with the emphasized vascular patterns of other visual predators, such as predatory birds and squamates, that support high metabolic requirements of orbital tissues (Parver, 1991; Barbour et al. 2002; Porter, 2015). The morphology of the eye (e.g. lens, retina, ganglion cells) is shaped by the properties of the visual field, the type of information gathered by the eye (e.g. edge or contrast enhancement), and ecological habits of each taxon (Cronin, 2005). Thus, ecological role (e.g. pursuit vs. ambush predator) may have an influence on the level of vascularization of the eye itself (i.e. retina) and its supporting structures. Indeed in birds, the orbital region is a well known site of thermal exchange (Pinshow et al. 1982) and it would be appropriate to test the hypothesis of a similar ability in crocodilians. Any evaporative cooling in the orbital region of crocodilians, including from the eyeball and eyelids, has several pathways to neurosensory tissues. Both arteries and veins form a vast plexus within the orbit, potentially allowing heat exchange. The intrinsic veins of the eyeball, including the choroid and ciliary plexuses, drain blood toward the ophthalmotemporal vein and into the ocular plexiform ring, and then into the orbital vein. Any blood cooled in the orbit can flow through the orbital vein and into the cavernous sinus, where it would influence the temperature of at least the hypothalamic region of the brain, if not other parts (Fig. 14). The orbital region also receives blood from the nasal region through the anastomosis between
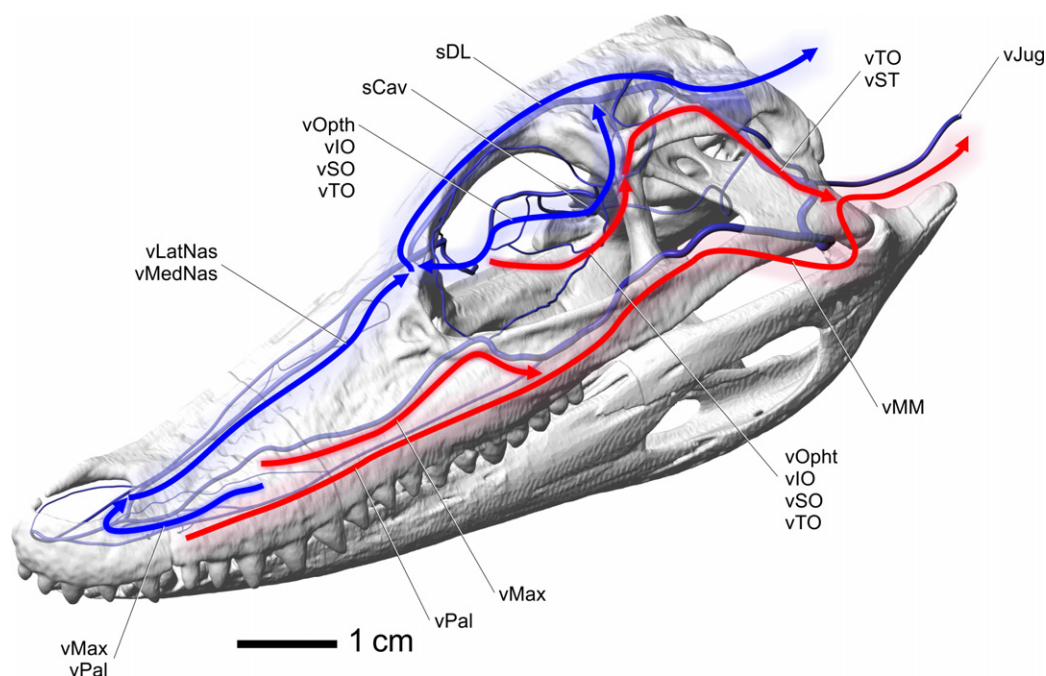
Fig. 14 *Alligator mississippiensis*, left rostrodorsolateral view, indicating possible pathways for blood to drain from sites of thermal exchange. Red arrows indicate pathways that likely have little influence on neurosensory tissues. Blue arrows indicate pathways that likely have an influence on neurosensory tissues. Labels indicate named blood vessels involved with indicated pathways. Vessel names: vMedNas, medial nasal vein; vLatNas, lateral nasal vein; sCav, cavernous sinus; sDL, dorsal longitudinal sinus; vJug, jugular vein; vMax, maxillary vein; vPal, palatine vein; vOphtd, dorsal branch of ophthalmotemporal vein; vOphtv, ventral branch of ophthalmotemporal vein; vIO, infraorbital vein; vSO, supraorbital vein; vTO, temporoorbital vein; vMM, maxillomandibular vein; vST, stapedial vein.

the nasal and ophthalmotemporal veins. This anastomosis can deliver cooled blood into the ocular plexiform ring and thus influence orbital tissue temperatures. The ophthalmotemporal vein is a tributary of the temporoorbital vein, at which point there is little potential for blood cooled from the orbital region to influence neurosensory tissues except through the caudal head vein.

The oral region offers a highly vascularized and large surface area along the bony secondary palate. The most direct route to the heart for blood from the palate is through the palatomaxillary veins, offering little influence on the temperature of neurosensory tissues because these veins ultimately drain directly to the jugular, bypassing the brain and eye regions (Fig. 14). The palatonasal anastomosis, however, does offer a pathway to neurosensory tissues. The oral region has been shown to influence head temperatures (Spotila et al. 1977; Smith, 1979), so there is a mechanism for cooled blood to be shunted around the head and not just drained into pathways that bypass neurosensory tissues. If venous drainage could be regulated by smooth muscles in the maxillary or palatomaxillary vein, as has been demonstrated in birds (Midtgård, 1984), blood flow could be shunted through the nasal region, where there would be a clear potential to influence the temperature of neurosensory tissues (Fig. 14). The anastomotic connections between the maxillary vein, palatine vein, lateral nasal vein, and

veins in the premaxilla, would allow blood to flow through and be cooled in the palatal plexus, then into the maxillary veins, then into the lateral nasal veins. This 'series mode' would allow blood from the palate to enter the nasal veins and then flow towards the brain and eyes. All of the blood in the ventral oral region (tongue, mandible), despite the tongue being a site of evaporative cooling, bypasses neurosensory tissues altogether and flows to the heart through the mandibular vein, then into the maxillomandibular vein, and into the jugular vein. This condition is also known in squamates (Porter & Witmer, 2015) and birds (Baumel, 1993).The role of the tongue in the thermoregulatory strategy of diapsids is currently not well understood. Especially since the crocodilian tongue has much more connective tissue and fat and less muscle than other diapsid tongues (Oelrich, 1956; Ferguson, 1981; Schwenk, 1986; Baumel, 1993; Delheusy et al. 1994).

The nasal region is another region with a previously unrecognized extensive vascular supply. The nasal region has been shown to be an important site of thermal exchange in birds (Midtgård, 1983, 1984); likewise, evaporative cooling that directly influences brain temperature has been demonstrated in the nasal region of squamates (Crawford et al. 1977). The use of the nasal cavity for thermoregulation in crocodilians has not been tested and is likely to be physiologically relevant. A large submucosal vascular

plexus is present on the dorsal and ventral aspect of the airway (Fig. 11), a plexus on the preconcha and concha indicates a rich evaporative surface for cooling to occur. The thermoregulatory significance of this much blood flowing around the airway has yet to be investigated but it is likely that it is biologically relevant. Additionally, a vast extracapsular vascular network involving the nasal gland and cavernous tissue within the nasal vestibule indicates the crocodilian nasal region is well vascularized, much more than was previously expected for an ectotherm. These findings may indicate that the nasal region is an important site of thermal exchange, in addition to the oral region, and perhaps even more important than the oral region, given that the nasal region has more direct venous drainage routes to the dural sinus system. Indeed, as discussed above, the oral region has been shown to have an influence on head temperature (Spotila et al. 1977; Smith, 1979), but the necessary route for this effect must be through the palatonasal anastomosis, potentially adding to the thermal importance of the nasal vasculature. The veins of these rich nasal plexuses drain into the medial and lateral nasal veins, which unite to form the nasal vein. The nasal vein then bifurcates, shunting blood along two routes. The medial route forms a tributary of the olfactory veins and dorsal longitudinal sinus, and the lateral route drains into the orbit via the supraorbital and ophthalmotemporal vein anastomosis. The nasal region is therefore in a position, with its large surface area, extensive blood flow, and patterns of venous drainage, to directly influence the temperature of both the brain and eye, potentially independently (Fig. 14). Once the cooled blood is in contact with the dural sinuses, the potential for whole brain cooling is present by cooling the intervening cerebrospinal fluid if not the neural tissue itself (Zenker & Kubik, 1996). This mechanism, in conjunction with venous drainage from the orbital region to the hypothalamic region, provides the anatomical 'plumbing' for selective brain temperature regulation, as well as an ability to regulate eyeball temperatures.

An important consideration in blood flow patterns is the location of venous valves. Discussion of venous valves in diapsids is largely limited to birds. Hossler & Olson (1984) and Hossler & West (1988) described venous valves in the orbits of ducks. Specifically, the valves of the salt gland and eyeball were described in detail using corrosion casting and electron microscopy. These two studies, unfortunately, did not provide much information beyond the orbit and only explicitly identified the infraorbital vein as containing valves.

The crocodilian encephalic vasculature that ultimately supplies the nasal region may reflect the upper limit of the ability of archosaur encephalic arteries to supply the nasal region. In birds, the rostral cerebral artery gives off the ethmoid artery, which is an important artery supplying the nasal region (Baumel, 1975, 1993; Porter & Witmer, 2016). During development, crocodilians show a similar condition to that of birds, with the rostral cerebral artery giving off the ethmoid artery, but the rostral cerebral artery also shares an anastomotic connection with the caudal cerebral artery (Burda, 1969). During development, the caudal cerebral artery progressively contributes more blood to the ethmoid artery, and the rostral cerebral artery obliterates its connection to the ethmoid artery (Burda, 1969).

Overall, the crocodilians in this sample demonstrated a fairly consistent and predictable vascular pattern that showed reliable osteological correlates observable in dried skulls. The larger arteries found at the base of the skull demonstrated the most variable branching patterns, the sites of thermal exchange being the least variable. The single crocodile in the sample was found to deviate little from the patterns found in multiple alligator specimens. The largest difference was related to its longirostrine condition when compared with alligators. These results may indicate that the thermoregulatory abilities of these two clades are very similar, at least on an anatomical level.

Unlike birds, the other extant archosaur group, extant crocodilians, demonstrate a universally aquatic life history and ectothermic physiology. It would then be valuable to investigate the physiological reasons why an ectotherm has the kinds of vascular thermoregulatory structures that are often associated with endothermy (highly vascular nasal conchae) and other structures associated with heat exchange (dense vascular plexuses in sites of thermal exchange, multiple retia mirabilia). These attributes could simply reflect their heritage more than their current habitus. Extinct archosaurs, basal to crown, have a rich history, including a large diversity of terrestrial forms, from taxa with large and powerful skulls such as *Postosuchus* (Chatterjee, 1985) to small-bodied, gracile basal crocodylomorphs such as *Junggarsuchus* (Clarke et al. 2004). A number of researchers have recently suggested that the more active, terrestrial ancestors of crocodilians may actually have been endothermic (Hillenius & Ruben, 2004; Seymour et al. 2004, 2012; Seymour, 2013) and may have deployed vascularized structures to better control body temperatures that were closer to lethal. Thus, the rich vascularization of sites of thermal exchange may be the result of crocodilian evolution, either as simply a trait held over from a terrestrial endothermic heritage or perhaps a modification of ancestral terrestrial thermoregulatory abilities for an aquatic lifestyle. Because of the known thermoregulatory abilities of both squamates (which have much more modest vascular thermoregulatory structures than crocodilians) and birds, the thermoregulatory abilities of crocodilians are likely underestimated. Whereas the *behavioral* thermoregulatory strategies of crocodilians are well known (e.g. sliding into the water when overheated; Smith, 1976, 1979; Drane et al. 1977; Smith et al. 1978, 1984; Fraser & Grigg, 1984; Franklin & Seebacher, 2003; Seebacher & Franklin, 2004, 2007), it is possible that the study of such behaviors may have resulted in more strictly *physiological* thermoregulatory strategies

being overlooked. The anatomical findings on blood flow though the nasal, oral, and orbital regions need to be investigated by experimental physiologists to determine the role and efficiency of evaporative cooling and its pathways to neurosensory tissues. Regardless of the crocodilian ability to physiologically thermoregulate, the benefit of behaviorally shuttling between land and water is still a precise control over the rate of heat gain and loss (Johnson, 1974; Smith, 1979; Seebacher, 1997) without expending resources on a physiological process. Yet the few papers that have looked into abilities of crocodilian physiological thermoregulation (Spotila et al. 1977; Smith, 1979) offer a hint that the physiological thermoregulatory abilities may indeed be at least on a par with, or surpass on some levels, the thermoregulatory abilities of their squamate and avian relatives.

Acknowledgements

Funding

Author contributions

References

Almeida L, Campos R (2011) A systematic study of the brain base arteries in the broad-snouted caiman (*Caiman latirostris*). *J Morphol Sci* **28**, 62–68.

Barbour HR, Archer MA, Hart NS, et al. (2002) Retinal characteristics of the ornate dragon lizard, *Ctenophorus ornatus*. *J Comp Neurol* **450**, 334–344.

Baumel JJ (1975) Aves: heart and blood vessels. In: *Sisson and Grossman's the Anatomy of the Domestic Animals* (ed. Getty R), pp. 1968–2003. Philadelphia: W.B. Saunders.

Baumel JJ (1993) Systema cardiovasculare. In: *Sisson and Grossman's the Anatomy of the Domestic Animals* (ed. Getty R), pp. 407–476. Philadelphia: W.B. Saunders.

Bellairs AA, Shute CCD (1953) Observations on the narial musculature of *Crocodilia* and its innervation from the sympathetic system. *J Anat* **87**, 367–380.

Bernstein MH, Sandoval I, Curtis MB, et al. (1979) Brain temperature in pigeons: effects of anterior respiratory bypass. *J Comp Physiol* **129**, 115–118.

Bourke JB, Porter WR, Ridgely RM, et al. (2014) Breathing life into dinosaurs: tackling challenges of soft-tissue restoration and nasal airflow in extinct species. *Anat Rec* **297**, 2148–2186.

Burda DJ (1969) Developmental aspects of intracranial arterial supply in the alligator brain. *J Comp Neurol* **135**, 369–380.

Chatterjee S (1985) *Postosuchus*, a new thecodontian reptile from the Triassic of Texas and the origin of Tyrannosaurs. *Philos Trans R Soc Lond B Biol Sci* **309**, 395–460.

Clarke JM, Xing X, Forster CA, et al. (2004) A Middle Jurassic 'sphenosuchian' from China and the origin of the crocodylian skull. *Nature* **430**, 1021–1024.

Colbert EH, Cowles RB, Bogert CM (1946) Temperature tolerances in the American alligator and their bearing on the habits, evolutions, and extinction of the dinosaurs. *B Am Mus Nat Hist* **86**, 327–374.

Crawford EC (1972) Brain and body temperatures in a panting lizard. *Science* **177**, 431–433.

Crawford EC, Palomeque J, Barber BJ (1977) A physiological basis for head-body temperature differences in a panting lizard. *Comp Biochem Physiol A Comp Physiol* **56A**, 161–163.

Cronin TW (2005) The visual ecology of predator-prey interactions. In: *Ecology of Predator-Prey Interactions* (eds Barbosa P, Castellanos I), pp. 105–138. New York: Oxford University Press.

Delheusy V, Toubeau G, Bels VL (1994) Tongue structure and function in *Oplurus cuvieri* (Reptilia: Iguanidae). *Anat Rec* **238**, 263–276.

Drane CR, Webb GJW, Heuer P (1977) Patterns of heating in the body trunk and tail of *Crocodylus porosus*. *J Therm Biol* **2**, 127–130.

Ferguson MW (1981) The structure and development of the palate in *Alligator mississippiensis*. *Arch Oral Biol* **26**, 427–443.

Franklin CE, Seebacher F (2003) The effect of heat transfer mode on heart rate responses and hysteresis during heating and

cooling in the estuarine crocodile *Crocodylus porosus. J Exp Biol* **206**, 1143–1151.

Fraser S, Grigg GC (1984) Control of thermal conductance is insignificant to thermoregulation in small reptiles. *Physiol Zool* **57**, 392–400.

Heath JE (1964) Head-body temperature differences in horned lizards. *Physiol Zool* **37**, 273–279.

Heath JE (1966) Venous shunts in the cephalic sinuses of horned lizards. *Physiol Zool* **39**, 30–35.

Hillenius WJ, Ruben JA (2004) Getting warmer, getting colder: reconstructing crocodylomorph physiology. *Physiol Biochem Zool* **77**, 1068–1072.

Hochstetter F (1906) Beiträge zur Anatomie und Entwicklungsgeschichte des Blutgefäßsystems der Krokodile. In: *Reise in Ostafrika in des Jahren 1903–1905*, vol. **4** (ed. Voeltzkow A), pp. 1–139. Stuttgart: E. Schweizerbartsche Verlagsbuchhandlung.

Holliday CM, Ridgely RC, Balanoff AM, et al. (2006) Cephalic vascular anatomy in flamingos (*Phoenicopterus ruber*) based on novel vascular injection and computed tomographic imaging analysis. *Anat Rec* **288A**, 1031–1041.

Holliday CM, Tsai HP, Skiljan RJ, et al. (2013) A 3D interactive model and atlas of the jaw musculature of *Alligator mississippiensis. PLoS One* **8**, e62806.

Hopson JA (1979) Paleoneurology. In: *Biology of the Reptilia, Volume 9, Neurology* (ed. Gans C), pp. 39–146. New York: Academic Press.

Hossler FE, Olson KR (1984) Microvasculature of the avian eye: studies on the eye of the duckling with microcorrosion casting, scanning electron microscopy, and stereology. *Am J Anat* **170**, 205–221.

Hossler FE, West RF (1988) Venous valve anatomy and morphometry: studies on the duckling using vascular corrosion casting. *Am J Anat* **181**, 425–432.

Johnson CR (1974) Thermoregulation in crocodilians – I. Head-body temperature control in the Papua-New Guinean Crocodiles, *Crocodylus novaeguineae* and *Crocodylus porosus. Comp Biochem Physiol A Mol Integr Physiol* **49A**, 3–28.

Kilgore DL, Bernstein D, Hudson DM (1976) Brain temperatures in birds. *J Comp Physiol* **110**, 209–215.

Martin BGH, Bellairs AA (1977) The narial excrescence and pterygoid bulla of the gharial, *Gavialis gangeticus* (Crocodilia). *J Zool* **182**, 541–558.

Midtgård U (1983) Scaling of the brain and the eye cooling system in birds: a morphometric analysis of the rete ophthalmicum. *J Exp Zool* **225**, 197–207.

Midtgård U (1984) Blood vessels and the occurrence of arteriovenous anastomoses in the cephalic heat loss areas of mallards, *Anas platyrhynchos* (Aves). *Zoomorphology* **104**, 323–335.

Mitchell D, Maloney SK, Jessen C, Laburn HP, Kamerman PR, Mitchell G, Fuller A. (2002) Adaptive heterothermy and selective brain cooling in arid-zone mammals. *Comp Biochem Phys B* **131**, 571–585.

Mitchell D, Maloney SK, Laburn HP, et al. (1997) Activity, blood temperature and brain temperature of free-ranging springbok. *J Comp Physiol* **167**, 335–343.

Montefeltro FC, Andrade DV, Larsson HCE (2016) The evolution of the meatal chamber in crocodyliforms. *J Anat* **228**, 838–863.

Oelrich TM (1956) The anatomy of the head of *Ctenosauria pectinata* (Iguanidae). *Misc Pub Mus Zool* **94**, 1–122. Ann Arbor: University of Michigan.

Parver LM (1991) Temperature modulating action of choroidal blood flow. *Eye (Lond)* **5**, 181–185.

Pinshow B, Bernstein MH, Lopez GE, et al. (1982) Regulation of brain temperature in pigeons: effect of corneal convection. *Am J Physiol* **242**, 577–581.

Porter WR (2015) Physiological implications of dinosaur cephalic vascular systems. Doctoral thesis, Ohio University.

Porter WR, Witmer LM (2015) Vascular patterns in iguanas and other squamates: blood vessels and sites of thermal exchange. *PLoS One* **10**, e0139215.

Porter WR, Witmer LM (2016) Avian cephalic vascular anatomy, sites of thermal exchange, and the rete ophthalmicum. *Anat Rec (Hoboken)* doi: 10.1002/ar.23375.

Pough FH (1980) Blood oxygen transport and delivery in reptiles. *Am Zool* **20**, 173–185.

Rathke H (1866) *Untersuchungen über die Entwickelung und den Körperbau der Krokodile* (ed. von Wittich W). Braunschweig: F. Vieweg und Sohn.

Reese AM (1914) The vascular system of the Florida alligator. *Proc Natl Acad Sci Philos* **66**, 413–425.

Reese AM (1915) *The Alligator and Its Allies*. New York: G.P. Putnam's Sons.

Schwenk K (1986) Morphology of the tongue in the tuatara, *Sphenodon punctatus* (Reptilia: Lepidosauria), with comments on function and phylogeny. *J Morphol* **188**, 129–156.

Sedlmayr JC (2002) Anatomy, evolution, and functional significance of cephalic vasculature in Archosauria. Doctoral thesis, Ohio University.

Sedlmayr JC, Witmer LM (2002) Rapid technique for imaging the blood vascular system using stereoangiography. *Anat Rec* **267**, 330–336.

Seebacher F, Grigg GC (1997) Patterns of body temperature in wild freshwater crocodiles, *Crocodylus johnstoni*: Thermoregulation versus thermoconformity, seasonal acclimation, and the effect of social interactions. *Copeia* **3**, 549–557.

Seebacher F, Franklin CE (2004) Integration of autonomic and local mechanisms in regulating cardiovascular responses to heating and cooling in a reptile (*Crocodylus porosus*). *J Comp Physiol B* **174**, 577–585.

Seebacher F, Franklin CE (2007) Redistribution of blood within the body is important for thermoregulation in an ectothermic vertebrate (*Crocodylus porosus*). *J Comp Physiol B* **177**, 841–848.

Seebacher F, Grigg GC, Beard LA (1999) Crocodiles as dinosaurs: behavioral thermoregulation in very large ectotherms leads to high and stable body temperatures. *J Exp Biol* **202**, 77–86.

Seymour RS (2013) Maximal aerobic and anaerobic power generation in large crocodiles versus mammals: implications for dinosaur gigantothermy. *PLoS One* **8**, e69361.

Seymour RS, Bennett-Stamper CL, Johnston SD, et al. (2004) Evidence for endothermic ancestors of crocodiles at the stem of archosaur evolution. *Physiol Biochem Zool* **77**, 1051–1067.

Seymour RS, Smith SL, White CR, et al. (2012) Blood flow to long bones indicates activity metabolism in mammals, reptiles and dinosaurs. *Proc Biol Sci* **279**, 451–456.

Smith EN (1976) Heating and cooling rates of the American alligator, *Alligator mississippiensis. Physiol Zool* **49**, 37–48.

Smith EN (1979) Behavioral and physiological thermoregulation of crocodilians. *Am Zool* **19**, 239–247.

Smith EN, Robertson S, Davies DG (1978) Cutaneous blood flow during heating and cooling in the American alligator. *Am J Physiol* **235**, R160–R167.

Smith EN, Standora EA, Robertson S (1984) Physiological thermoregulation of mature alligators. *Comp Biochem Physiol A* **77A**, 189–193.

Spotila JR, Terpin KM, Dodson P (1977) Mouth gaping as an effective thermoregulatory device in alligators. *Nature* **265**, 235–236.

Templeton JR (1960) Respiration and water loss at higher temperatures in the desert iguana, *Dipsosaurus dorsalis. Physiol Zool* **33**, 136–145.

Witmer LM (1995a) The extant phylogenetic bracket and the importance of reconstructing soft tissues in fossils. In: *Functional Morphology in Vertebrate Paleontology* (ed. Thomason JJ), pp. 19–33. New York: Cambridge University Press.

Witmer LM (1995b) Homology of facial structures in extant archosaurs (Birds and Crocodilians), with special reference to paranasal pneumaticity and nasal conchae. *J Morphol* **225**, 269–327.

Witmer LM (1997) The evolution of the antorbital cavity of archosaur: a study in soft-tissue reconstruction in the fossil record with an analysis of the function in pneumaticity. *J Vert Paleontol* **17**(Suppl 1), 1–75.

Zenker W, Kubik S (1996) Brain cooling in humans – anatomical considerations. *Anat Embryol* **193**, 1–13.

Supporting Information

Additional Supporting Information may be found in the online version of this article:

Fig. S1. A 3-Dimensional model of the skull and blood vessels of an alligator. To activate the model, click on the alligator skull. The alligator skull and blood vessels can be freely rotated and zoomed, structures can be made visible, invisible, or transparent. Blood vessels can be identified by clicking on them and looking to the bolded name at left in the Model Tree. In the center of the Model Tree, there is a list of views that orients the model to match the in-text figures.